Merging high-quality biochemical fractionation with a refined flow cytometry approach to monitor nucleocytoplasmic protein expression throughout the unperturbed mammalian cell cycle

Margit Rosner, Katharina Schipany & Markus Hengstschläger

Institute of Medical Genetics, Medical University of Vienna, Vienna, Austria. Correspondence should be addressed to M.H. (markus.hengstschlaeger@meduniwien.ac.at).

Published online 28 February 2013; doi:10.1038/nprot.2013.011

This protocol describes a method for nucleocytoplasmic protein tracking during normal cell cycle progression using unmanipulated, asynchronous cells. In contrast with prevalent traditional methods, our approach does not require time-consuming, perturbing cell synchronization or separation. To this end, we chose a single-cell approach and developed a flow cytometry assay that is applied to whole cells and isolated nuclei. Our protocol involves a stepwise biochemical fractionation procedure to purify nuclei from whole cells, conventional DNA and indirect immunostaining techniques for the dual labeling of cells and nuclei for DNA and protein, and a refined concept of flow cytometric data processing and calculation: through the specific combination of DNA and cell size analyses, G1, S and G2/M phases of the cell cycle are further dissected to establish a high-resolution map of cell cycle progression, to which protein expression in cells or nuclei is correlated. In a final data analysis step, cell cycle–related, cytoplasmic protein expression is calculated on the basis of results obtained for whole cells and isolated nuclei. A minimum of 8 h is required to complete the procedure. As the approach does not require cell type–restricting pretreatments, numerous cell types of different origin can be readily studied. Human amniotic fluid stem cells, primary human fibroblasts, immortalized mouse fibroblasts and transformed tumor cells are analyzed at comparable efficiencies, demonstrating low intercell assay variability.

INTRODUCTION

Spatiotemporal control of cellular signaling

Simple models of linear signal transduction evolving into complex networks reflect the key discoveries in today's signaling research. In addition to the identification and functional alignment of signaling components, evaluation of their spatiotemporal control is of major importance for the overall understanding of signaling events. The coordinated regulation of signaling proteins in space and time ensures that molecular and functional interactors come together where and when they need to. Compartmentalization of proteins in near proximity, their changes in expression over time and their interaction in order to form dynamic signaling scaffolds are important regulatory mechanisms that define signaling specificity and diversity, and which constitute an important rate-limiting step in overall signaling capacity. Thus, the spatiotemporal control of signaling proteins is a prerequisite for the proper coordination of signaling events, and defects are inevitably coupled to states of disease[1–3].

Accordingly, the identification of specific spatiotemporal patterns within a signaling cascade and the elucidation of their underlying molecular mechanisms are of high relevance for the in-depth understanding of particular signaling events and can provide a novel platform for diagnosis and therapy. Spatiotemporal profiling of tumor-derived material, as well as the knowledge of the cell cycle phase specificity of antitumor drugs or their putative effects on the subcellular redistribution of target proteins, may be of unpredictable value in designing highly specific antitumor strategies to redirect unguided signaling[4–6].

Nucleocytoplasmic protein tracking throughout the cell cycle

Development of the protocol. The mechanistic target of rapamycin (mTOR), a serine/threonine kinase involved in the regulation of cell growth, is the prototype of a signaling molecule of which knowledge of downstream effectors and upstream regulators has rapidly expanded within a few years of research[7]. Traditional biochemical approaches involving the genetic and pharmacologic modulation of key signaling molecules, as well as sophisticated screening methods, were used to identify and functionally assemble the major players within this important signaling cascade. Although myriad mTOR signaling components have been identified[7], an understanding of their spatiotemporal control is lagging behind. We developed this protocol to gain insights into the regulation and interplay of mTOR signaling molecules in space (nucleocytoplasmic distribution) and time (ongoing cell cycle). We previously investigated the nucleocytoplasmic distribution of major mTOR signaling components in primary human cells[8]. Since then, the importance of localization studies has been increasingly appreciated, and major progress in the understanding of mTOR shuttling between intracytoplasmic compartments and the formation of cytoplasmic signaling scaffolds and circuits has been made[7]. However, as varying but substantial amounts of mTOR were found to be localized to the nucleus, coevaluation of the nuclear compartment is essential. The nucleus is a major signaling compartment and was identified as being a relevant target of tumor-associated changes[3]. Clarifying its role in accommodating or regulating mTOR activity is thus of high importance. This protocol centers on a rapid and proven biochemical fractionation approach that involves the basic steps of (i) hypotonic cell swelling, (ii) detergent-mediated cell membrane disruption and cell homogenization, (iii) separation of cytoplasmic extracts, (iv) purification of isolated nuclei and (v) extraction of soluble nuclear proteins (**Fig. 1**)[8,9]. This procedure is classically followed by an immunoblotting step to detect the particular protein of interest

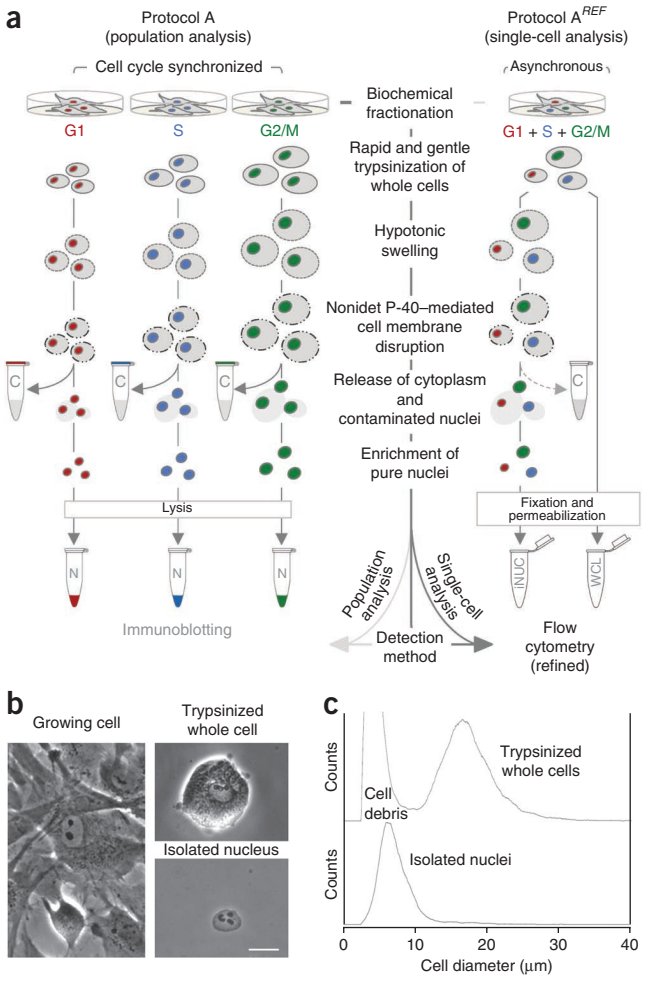

Figure 1 | Isolation of nuclei for use in traditional and improved cell cycle studies. (**a**) Outline of the stepwise fractionation procedure in the context of conventional (protocol A) and refined (protocol A^{REF}) assay design. For details on the procedure and the differences between protocols A and A^{REF}, see the INTRODUCTION. C, cytoplasm; iNUC, isolated nuclei; N, nucleus; WCL, whole cells. (**b**) Representative phase-contrast images of Q1 hAFS cells, either actively growing in a cell culture plate (left), trypsinized (right, top) or fractionated to obtain nuclei of high purity and integrity (right, bottom). Scale bar, 10 µm. (**c**) Size distribution analyses of nonfixed, nonpermeabilized whole cells and isolated nuclei using a CASY cell counter and analyzer.

in obtained fractions (**Fig. 1a**, protocol A)[8]. As an initial improvement, we aimed to investigating the protein's nucleocytoplasmic distribution in relation to cell cycle progression to identify putative cell cycle–regulated events. With respect to cell cycle distribution, cultures of exponentially growing cells are generally asynchronous, with each cell passing through the cycle independently of the cell cycle stage of its neighboring cells. However, classic western blotting takes the average of many cells, providing a single data point for the whole population of cells. Accordingly, when sticking to the immunoblotting detection step, prior cell cycle synchronization of cells is necessary.

Traditionally, synchronous progression through the cell cycle is generated by reversibly arresting cells at a particular stage of the cell cycle (block), followed by removing the block, thus allowing cells to resume division (release). By using a proven serum starvation/re-stimulation approach followed by the aforementioned fractionation procedure and a final immunoblotting step (**Fig. 1a**, protocol A), we recently identified very specific spatiotemporal patterns in the expression of mTOR and its downstream effector p70S6K1 (**Fig. 2**)[10,11].

The utility of our fractionation protocol to obtain nuclei of high purity and integrity was proven in various different studies (**Figs. 1b**,**c** and **2a**,**b**)[8–11] and tempted us to seek a modification of the protocol that would allow further improvement of our methodology. As the final detection method determines the need for prior cell cycle synchronization, we decided to exchange the immunoblotting step (population analysis) for a flow cytometry approach (single-cell analysis). One of the fundamentals of flow cytometry is its ability to measure multiple properties of individual cells in a single step. By using well-established DNA and antibody staining techniques, it is possible to obtain information on the abundance of a protein in relation to cell cycle progression by correlating its expression with the cell's position in the cycle[12–15]. However, traditional flow cytometry to obtain cell cycle stage–dependent patterns of protein expression has two principal shortcomings: (i) As protein expression is correlated to the DNA content, time-dependent resolution of the G1 and G2/M phases of the cell cycle is not possible. (ii) Proven protocols for flow cytometric DNA and protein correlations are limited and do not include the coanalysis of isolated nuclei to study protein localization. Accordingly, and as a final improvement, we adapted conditions for the efficient staining of isolated nuclei for use in flow cytometry and designed a new strategy for flow cytometric data analyses, which we call 'a refined flow cytometry approach'. The sum of the biochemical fractionation approach and the modifications described above yields an improved protocol for nucleocytoplasmic protein tracking throughout the ongoing cell cycle using asynchronous, unmanipulated cells (**Fig. 1a**, protocol A^{REF}). By using this protocol, we could not only recapitulate and expand the basic spatiotemporal pattern of mTOR expression identified earlier (**Fig. 2b–d** and ANTICIPATED RESULTS), but also recently provided first insights into the phosphorylation of nuclear and cytoplasmic pools of the mTOR effector ribosomal protein S6 during unhalted cell cycle progression[16].

Principle of the method

The basic principle of our approach exploits the particular relationship between a cell's size and its specific position in the cell cycle. It involves the combination of flow cytometric DNA and cell size analyses to establish a high-resolution map of continuous cell cycle progression, to which protein expression, evaluated via simultaneous protein stainings, is correlated. Applied to whole cells and isolated nuclei, obtained data sets are mathematically processed to generate data on the corresponding cytoplasmic regulations. The final pattern is representative of the protein's specific spatiotemporal distribution.

A single cell passing through the ongoing cell cycle harbors two characteristic properties: at each time point during the cycle, a cell has a defined content of DNA and a particular size. During cell cycle progression, cell size increases to allow a cell to divide into two daughter cells. Thus, between cell divisions there is a continuous variation in cell size. Early G1 cells are approximately half the size of cells in the late G2 or M phase, S-phase cells are intermediate in size and early G1–phase cells are smaller than late G1–phase cells[17,18].

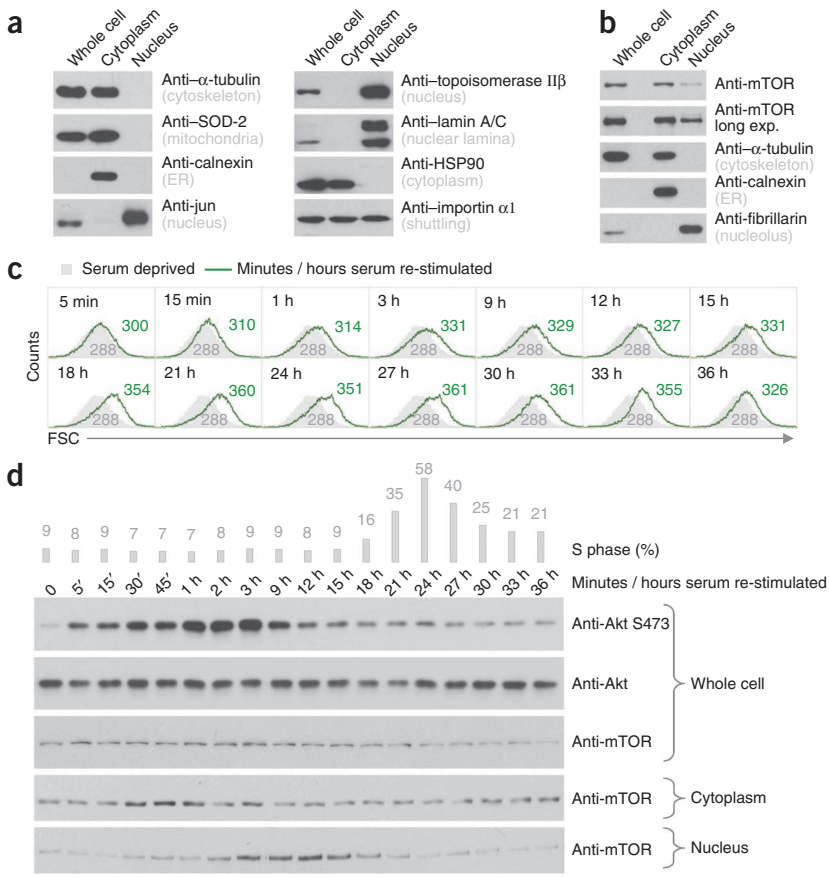

Figure 2 | Nucleocytoplasmic protein tracking throughout the cell cycle via traditional immunoblotting. (**a**) Immunoblot analyses of subcellular marker proteins as indicated to verify the purity of cytoplasmic and nuclear fractions. Whole-cell lysates were examined in parallel and equal amounts of protein were loaded for each fraction. ER, endoplasmic reticulum. (**b**) Immunoblot analyses of the nucleocytoplasmic localization of mTOR in asynchronously growing primary human fibroblasts. (**c**) Flow cytometric cell size analyses of G0/G1 synchronized (serum deprived) and released (serum re-stimulated) primary human fibroblasts at indicated time points. Corresponding FSC histograms and means are presented. (**d**) Top, flow cytometric DNA content analyses of cells described in **c**. The percentage of cells in S phase is indicated. Bottom, immunoblot analyses of the nucleocytoplasmic localization of mTOR in synchronized and released cells described in **c**. Whole-cell lysates were examined in parallel for indicated proteins. Panel **a** is reprinted from ref. 10; panels **b**–**d** are modified and reprinted from ref. 11.

Essential to our approach is the fact that the cell cycle–dependent increase in nuclear size is proportional to the increase in total cell size[19,20]. Thus, cell or nuclear size can be used as a reliable parameter to monitor continuous cell cycle progression. In combination with DNA content analyses, cell size analyses allow the in-depth and time-dependent resolution of G1 and G2/M phases of the cell cycle. Flow cytometric forward scatter (FSC) analyses as a relative measure of cell size are well established, and they are widely used in combination with DNA content analyses (albeit for another purpose and in another design), especially in growth signaling research (**Box 1**). **Figure 3** illustrates the principle and the main steps of the refined flow cytometry approach: after biochemical fractionation, pure, intact nuclei and whole cells derived from the same pool of cells are stained for DNA and a particular protein of interest. After acquisition on the cytometer, obtained data sets are analyzed in a four-step procedure involving (i) the initial gating for G1, S and G2/M subsets, followed by (ii) their specific dissection using FSC (G1; G2/M) and DNA (S) parameters to establish a map of continuous cell cycle progression, (iii) the correlation of obtained FSC/DNA subsets with the corresponding signals of the protein staining and (iv) a final step of data calculation to subtract nuclear from whole cell results to obtain data on the corresponding cytoplasmic regulation.

Comparison with other methods

In contrast to our approach, the largely unrivaled, traditional immunoblotting approaches to study cell cycle–related events require prior cell synchronization. Numerous methods for mammalian cell cycle synchronization exist (**Table 1**) and are associated with specific pros and cons[21–25]. The major criticism concerns the utility of synchronization procedures to produce cell populations reflecting cells during the normal cell division cycle and not those recovering from the stress or artifacts of synchronization.

The classic arrest/release strategy involving the single or combined administration of chemical inhibitors acting at various points throughout the cell cycle is often the primary method of choice: inhibitors are generally effective in a wide variety of different cell types, do not require special equipment, are simply added to the culture medium and are very economical. However, compared with all other available methods, the use of synchronization drugs is associated with the most severe concerns: for many of them, the mode of action is still not fully understood, bearing the risk of having more than one target in the cell; they have been shown to induce growth imbalance and stress responses and generally lead to severe perturbations of the cellular steady state[26–29]. The method of classic serum deprivation/re-stimulation, which reflects the normal pattern of cell growth (**Fig. 2c**), is one of the most commonly used synchronization approaches. Although it allows drawing very specific conclusions (e.g., on the exit of G0 to G1), it may have some limitations. (i) The efficiency of the method depends on the susceptibility of cells to exit into G0 after serum withdrawal. G0 arrest is hard to achieve in transformed cells, as their proliferation potential is less dependent on the presence of serum and growth factors. Other cells may exhibit decreased viability under low serum conditions. (ii) Exit from G0 into G1 does not reflect G1 progression of actively cycling cells after the completion of mitosis. A substantial amount of serum-inducible genes is coevaluated ('serum response'). (iii) Serum re-stimulation of G0-arrested cells leads to reasonable synchrony during progression through G1 and at the G1/S transition, but rapidly declines as cells progress further through G2 and M. (iv) Depending on the cell type, the induction of quiescence requires different periods of time. Thus, careful optimization of

Box 1 | FSC-based cell sizing and its use in growth signaling research

How does FSC relate to cell size? Basically, light scattering occurs when a particle deflects incident light. Cells, either labeled with a specific fluorophore or unlabeled, scatter light at all angles when passing through a laser beam. By definition, the FSC (or low-angle light scatter) is a measurement of mostly diffracted light, which is detected in the forward direction at a limited angular range (approximately 1°–10°) as the laser light strikes the cell. This light is received by a detector that converts the recorded intensity into a voltage pulse, which in turn can be used to quantify the parameter. The magnitude of forward scatter or voltage pulse is roughly proportional to the relative cell-surface area or size of the cell[93]. One of the earliest and most widespread applications of flow cytometric FSC analyses in basic science was the discrimination of live and dead cells on the basis of their characteristic differences in cell size. In combination with other methods, this approach is still used in apoptosis research[94,95]. The true benefit of FSC evaluation, however, is the fact that it can be correlated with numerous other parameters at the single-cell level during multiparameter flow cytometry. Most relevant to any assay that evaluates cell size in a population of asynchronously growing cells is the simultaneous assessment of cell size and DNA content. As cells continuously grow during cell cycle progression, cells in the G1 phase of the ongoing cell cycle are smaller than cells in S or G2/M. Thus, a decrease in a population's size distribution (e.g., upon treatment with a particular agent) may be either due to a true, growth-inhibitory effect that renders all or some of the cells smaller or may simply reflect differences in the cell cycle distribution owing to a cell cycle inhibitory effect (e.g., arrest of cells in G1 with an increase in the amount of small cells and a concomitant decrease in the amount of larger cells). When paralleled by a cell cycle–deregulating effect, FSC analyses of G1, S and G2/M subsets are therefore essential to specifying a putative size effect. Modulation of mTOR as a major growth-regulating kinase is well known to trigger both, cell size and cell cycle effects. Numerous studies involving multiple different approaches to modulate mTOR expression and function have used and are still using this proven approach of FSC/DNA correlation to establish the role of mTOR and mTOR-associated proteins in cell size regulation[96–102]. Apart from this application of separating cell size from cell cycle effects, the connection of FSC and cell cycle progression can also be drawn at other, more subtle levels: although the specific DNA content of the cell is a very precise measure of cell cycle progression, simultaneous FSC measurements allow to monitor cell cycle progression in more detail. In this respect, the FSC was demonstrated to be a very sensitive parameter to follow G1 progression of G0/G1 synchronized and released cells during the first hours of serum re-stimulation when cell cycle progression is not yet evident at the level of DNA (**Fig. 2c**)[11]. The idea of shifting this approach of correlated DNA/FSC analyses from a population of synchronized cells to a population of asynchronously growing cells was finally verified in the protocol presented here: Cells in the G1 and G2/M phases of the cell cycle, for which a time-dependent resolution via DNA content analyses is not possible, are further analyzed according to the increase in cell size (FSC) during cell cycle progression, thus providing information on early to late stages of the specific cell cycle phase.

both the amount of serum withdrawn and the length of withdrawal, as well as the proper adjustment of seeding densities, is necessary (**Table 1** and references therein)[21–23].

Similar to our approach, the technique of centrifugal elutriation makes use of the continuous increase in cell size as cells travel through the cycle. Eliminating the need for any exogenous treatments to artificially induce synchrony, asynchronous populations of actively cycling cells are separated according to their sedimentation velocity, which is proportional to their size. Although unmanipulated cells of all cell cycle phases, including intermediate states, can be isolated, some substantial shortcomings exist: the elutriation process, during which the cells are kept floating in the elutriation chamber and do not further progress through the cycle, usually takes hours. Stress responses that induce changes in the cell's signaling status are very likely to occur. Notably, separation efficiency and quality have been shown to depend on the cell type studied. Thus, substantial intercell variability has to be encountered. The need for a relatively large amount of cells, special equipment and the experienced users are additionally limiting. The staining of live cells with DNA-binding dyes, followed by flow cytometry and cell sorting can result in similar problems, including adverse effects due to extended separation times and antibody/ligand/dye-mediated perturbations (**Table 1** and references therein)[25].

Collectively, current implementations for producing cell synchrony have specific benefits, but they tend to perturb the cellular steady state to varying extents. The use of more than one synchronization approach to prove or exclude a putative cell cycle–regulated event would be a reasonable possibility to verify obtained results (this protocol)[30–32].

The sum of all the mentioned drawbacks of cell cycle synchronization is the overriding advantage of our modified single-cell approach. At the same time, there are several pros to flow cytometric single-cell analysis. (i) The number of cells required for analysis is low. (ii) Flow cytometric signals can be acquired in the logrithmic scale (up to 10^4), and they do not show saturation and thus can be reasonably quantified[13,14]. (iii) Depending on the configuration of the flow cytometer, multiple parameters (including protein phosphorylation) can be coevaluated in a single step, allowing comprehensive sample profiling. (iv) Extended sample preparation times are typically not required, and the whole procedure can be completed within a minimum of 8 h. (v) As sample preparation is limited to DNA and antibody staining techniques, increased intercell variability can be largely excluded.

The feasibility of using isolated nuclei in flow cytometry applications is a prerequisite for our assay and has been extensively proven (see ANTICIPATED RESULTS). Including the modification of specific FSC and DNA analyses, our method displaces existing (albeit rare) approaches to flow cytometric DNA versus protein analysis[15]. Our assay may be only rivaled by automated time-lapse microscopy and image quantification approaches, which are limited in the number of cells that can be analyzed; they also require special equipment and are often restricted to trained users of core facilities, thereby excluding the possibility of flexible practice by the end user. The application of our protocol, however, only requires a standard

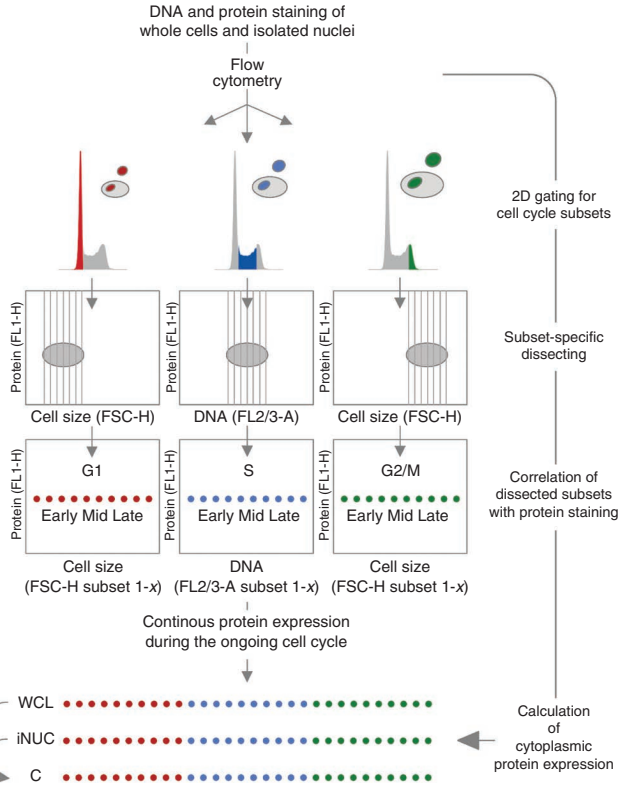

Figure 3 | Refined approach of flow cytometric data analysis. After DNA and protein staining and flow cytometric data acquisition, whole cells (WCL) and isolated nuclei (iNUC) are finally analyzed via a refined approach of data processing. Illustrated are the main steps of the gating procedure to obtain a high-resolution map of cell cycle progression, to which whole cell and nuclear protein expression is correlated. During the last step of data analysis, cytoplasmic (C) protein expression is calculated on the basis of results obtained for whole cell and isolated nuclei. For details see the INTRODUCTION. Subset 1-*x* indicates FSC or DNA subset number 1 to variable *x* (total number of gated subsets depends on cell types and total numbers of cells analyzed).

benchtop cytometer, equipped with lasers and filters for standard applications (see MATERIALS).

Taken together, our evolved approach entirely avoids any chemically, environmentally or mechanically induced cellular stresses in order to induce cell synchrony. Putative perturbations due to biochemical fractionation have been kept to a minimum by falling back to a widely proven protocol[8–11]. Thus, we conclude that this protocol does not merely expand the list of available methods but provides a rational, stand-alone alternative for identifying spatiotemporal patterns of protein expression in a way that is not possible with any other method.

Applications of the method

Numerous cells and cell lines, ranging from primary human cells (human amniotic fluid stem (hAFS) cells; nonimmortalized, nontransformed diploid fibroblasts) to immortalized mouse embryonic fibroblasts (MEFs) and transformed tumor cells, were tested during the setup of this protocol and can be analyzed for the cell cyle–dependent nucleocytoplasmic distribution of a particular protein of interest (see MATERIALS and ANTICIPATED RESULTS). The main applications of our method thus arise from the advantages when compared with traditional approaches as outlined above, and from the fact that our approach is not restricted to the analysis of a limited number of cell types. Owing to its feasibility, this approach may be a valuable tool for high-throughput and screening analyses, allowing one to establish a spatiotemporal map of a whole signaling cascade under identical experimental conditions. In combination with methods for modulating gene expression, such as RNA interference approaches, these correlative patterns can be functionally elucidated to identify key players of spatiotemporal control. As prior cell synchronization is avoided, even cell cycle regulatory proteins themselves can be investigated for their putative effects on the cell cycle regulation of their downstream targets. Finally, various approved drugs and small-molecule inhibitors can be tested for their effect on identified patterns in order to expand our knowledge of their mode of action and their use in particular therapies[5,6].

Because intercell variability in this assay is low, prior synchronization or even cell culturing is not required and only a low number of cells is needed for analysis, this assay allows the direct comparison of primary cells of different origins or entities with different proliferative or biochemical properties. To understand how particular regulatory processes become altered in cells as they progress from normal cells to tumor cells, spatiotemporal phenotyping of freshly isolated tumor samples and their corresponding normal counterparts may be a valuable approach to detect differences, reveal targets and survey the response to particular drugs. Advanced technical approaches for the preparation of solid tumor masses, biopsies and tissues for use in flow cytometry are available and could be explored for their compatibility with high-quality biochemical fractionation[13,14].

Experimental design

Basic considerations before starting. This procedure was optimized using monoclonal hAFS cells, for which we previously established a very efficient, lipid-based siRNA transfection protocol[33,34]. The following step-by-step protocol describes the detailed conditions for these particular cells, but in our experience virtually any cells of interest can be analyzed in this assay. The only rate-limiting step to be considered is the feasibility of cells for biochemical fractionation. We evaluated multiple cell lines during the setup of this method, with the majority being successfully used overall. We observed only minor qualitative differences, primarily affecting the purity of isolated nuclei. Tested cells and cell lines include human nontransformed, nonimmortalized IMR-90 fibroblasts, HeLa human cervical carcinoma cells, immortalized MEFs (either wild type or knocked out for several different genes) and BxPC-3 human pancreas carcinoma cells (**Fig. 2**, MATERIALS, ANTICIPATED RESULTS and data not shown)[8,1011].

During the initial setup of this protocol in the laboratory, we recommend starting with exponentially growing cells harboring a diploid DNA content. A population of cells with a cell cycle distribution of 50–55% G1-phase cells, 30% S-phase cells and 15–20% G2/M-phase cells cytofluorometrically yields clearly distinguishable DNA subsets that facilitate proper gating and thus allow the discrimination of cell cycle phases during the first, basic steps of data analysis (**Supplementary Figs. 1–4**).

Reading and applying this protocol requires some basic knowledge of how a flow cytometer works, and of how to handle and perform the basic steps of data acquisition and analysis (e.g., software-based creation of analysis plots). This assay was established on a FACSCalibur (Becton Dickinson) benchtop cytometer, a basic

TABLE 1 | Common methods for mammalian cell cycle synchronization.

Whole-culture (or whole-batch) synchronization methods

Method				
Basic approach	**Synchrony inducing agent or treatment**	**Proposed mechanism of action**	**Cell cycle stage blocked**	**References**
Chemical/pharmacological inhibition of DNA replication/synthesis *or* mitotic spindle formation	Lovastatin	Inhibition of HMG-CoA reductase (cholesterol synthesis) and the proteasome	(Early) G1	41–44
	Mimosine	Inhibition of thymidine, nucleotide biosynthesis, inhibition of Ctf4/chromatin binding	Late G1; G1/S	45–48
	Thymidine	Excess thymidine-induced feedback inhibition of DNA replication	G1/S	24,37,49–52
	Aphidicolin	Inhibition of DNA polymerase-α and DNA polymerase-δ	G1/S	53–55
	Hydroxyurea	Inhibition of ribonucleotide reductase	G1/S	32,40,56–58
	Colchicine/colcemide	Inhibition of microtubule polymerization	G2/M	59–62
	Nocodazole	Inhibition of microtubule polymerization	G2/M	24,63–66
Mitogen or growth factor withdrawal	Serum starvation	Growth restriction–induced quiescence	G0/G1	10,11,30,31,67–71
	Amino acid starvation	Growth restriction–induced quiescence	G0/G1	51,72–74
Density arrest	Contact inhibition	Cell-cell contact–induced activation of specific transcriptional programs	G1	75–78

Cell separation methods

Method				
Basic approach	**Technique**	**Main principle**	**Cell cycle stage isolated**	**Reference**
Mechanical separation on the basis of cell adhesion properties	Mitotic shake-off	Dislodgment of low adhesive, mitotic cells by agitation	M	79–82
Physical separation on the basis of cell size and to a lesser extent density	Countercurrent centrifugal elutriation (CCE)	Separation of cells according to their sedimentation velocity in a gravitational field where the liquid containing the cells is made to flow against the centrifugal force with the sedimentation rate of cells being proportional to their size	G1, S, G2/M and intermediate states (up to 12 fractions)	30,31,83–88
Physical separation based on specific intracellular (e.g., DNA content) and cell surface/size properties	Flow cytometry and cell sorting	Characterization of cells according to antibody/ligand/dye-mediated fluorescence and scattered light in a hydrodynamically focused stream of liquid with subsequent electrostatic, mechanical or fluidic switching sorting	G1, S, G2/M	89–92

instrument for standard applications. Sample acquisition in the course of a two-color setup like the one described here is basically performed by following standard procedures. As the actual improvement of our assay is linked to a new approach to flow cytometric data processing and analysis (**Figs. 1a** and **3**), steps of data acquisition are roughly outlined while data analysis and calculation are described in more detail.

Recommended experimental controls, including the application of fractionation controls, basic controls for flow cytometry, the analysis of control proteins known to exert (or to be devoid of) cell cycle–dependent expression and/or localization and information on general validity check, are separately outlined in each section of the PROCEDURE, are discussed in the RESULTS section and are included in **Figures 1–7** and **Supplementary Figures 1–12**.

Detachment and preparation of adherent cells for fractionation (Steps 1–12). Trypsinization is the method of choice for detaching adherent cells for subsequent flow cytometric DNA analyses, and it is an excellent method for isolating intact, single cells for use in biochemical fractionation approaches. As the proteolytic cleavage of cell adhesion proteins and its putative downstream effects may be associated with mild perturbations, care was taken in establishing a rapid and gentle trypsinization protocol that is carried out room temperature (20–25 °C) and that was previously proven to affect neither the expression level nor the phosphorylation status of analyzed signaling proteins[10]. Detachment by physical means (e.g., cell scraping) is not recommended, as this may lead to reduced membrane integrity, unreliable cell size analyses and loss of material for subsequent fractionation.

Isolation of pure, intact nuclei via biochemical fractionation (Steps 13–24). The trypsinization steps of the protocol have already been established and have been widely used to generate cytoplasmic and nuclear fractions of high purity using numerous cells of various origin (see MATERIALS and ANTICIPATED RESULTS)[9–11]. Moreover, this protocol turned out to be extremely versatile in that minor modifications (e.g., substitution of a particular detergent) could be introduced to meet very specific, context-dependent demands[8]. It is important to stress that this approach entirely fulfills the stringent criteria of nuclear purity, integrity and yield that have proven to be essential for the successful outcome of this procedure.

Fixation and permeabilization of whole cells and isolated nuclei (Steps 25–31). After testing different fixation and permeabilization conditions for whole cells and isolated nuclei (**Supplementary Fig. 1** and data not shown), the protocol below (a broadly applicable combination of formaldehyde and methanol)[14] was finally adopted for its ability to provide adequate results for the simultaneous staining of DNA and protein, its feasibility, and its optimal staining efficiency for almost all tested antibodies.

Protein and DNA staining of whole cells and isolated nuclei (Steps 32–45). For immunostaining of intracellular proteins, an indirect approach using unconjugated primary antibodies and fluorochrome-labeled secondary antibodies is preferred over a direct labeling system for several reasons. (i) When carefully chosen, unconjugated primary antibodies can be used in many distinct applications (e.g., western blotting, immunoprecipitation, immunofluorescence, flow cytometry). This allows one to very efficiently substitute one method for another or to switch between different methods. With respect to laboratory resources, this is a very economical approach. (ii) Although single-cell analysis via flow cytometry has numerous advantages over other approaches (as specifically outlined in this protocol), its application requires extraordinary effort and accuracy in verifying the specificity of the used antibodies. In our experience, false positive results are very likely to occur but can be limited to a minimum when applying a combination of knockout, knockdown and pharmacological inhibition approaches to prove antibody specificity. Even known differences in an antibody's species reactivity can be exploited for this purpose (**Supplementary Figs. 5–7**). The use of an unconjugated primary antibody allows the additional evaluation of its specificity via immunoblotting by analyzing the molecular weight of the target protein and (to some degree) evaluating the extent of background staining, an extremely valuable option restricted to western blotting (**Supplementary Fig. 5b**). (iii) Multiparameter analysis, as a fundamental concept of flow cytometry, enables the simultaneous assessment of multiple proteins in one single reaction. The use of unconjugated primary antibodies therefore offers the possibility of detecting the protein of interest via different fluorescent labels, which in turn allows the use of multiple distinct antibody combinations to meet specific demands.

As with any other method, but especially for flow cytometric approaches as the one described here, prior evaluation of antibody specificity is crucial. Reliable discrimination between positive and negative signals is essential in order to clearly distinguish weakly positive stainings (e.g., proteins with low, nuclear abundance) from nonspecific stainings. As outlined above, deliberate preliminary experiments (e.g., antibody titrations) are thus suggested to be performed (**Supplementary Figs. 5** and **6**). In the particular experiment, proper controls to be coanalyzed along with the sample of interest include (i) species- and subtype-matched control antibodies (isotype controls) and more stringent (ii) cells lacking the protein of interest (knockout cells), either separately coanalyzed or spiked earlier into the test population (**Supplementary Fig. 5b–d**). These considerations must be included when planning the overall amount of starting material needed. This protocol covers the coanalysis of one isotype control per specific antibody per population (whole cells and isolated nuclei, respectively).

Data acquisition on the flow cytometer (Steps 46–53). Basically, stained cells or nuclei are acquired with the BD (Becton Dickinson) CellQuest Pro 6.0 software at medium flow rate on a FACSCalibur benchtop cytometer equipped with 488-nm (blue argon) and 635-nm (red diode) lasers and emission filters for FITC (FL1), phycoerythrin (PE; FL2), Cy5-PE (FL3) and allophycocyanin (APC; FL4) (BD Biosciences). In theory, this instrument configuration allows one to simultaneously measure as many as six separate parameters on each cell that passes through the laser beam. These are two scattered-light parameters, FSC and SSC (side scatter), and four emitted-light (fluorescence) parameters (FL1-4). Our protocol (based on a two-color approach) involves four parameters for data acquisition and analysis: FSC, SSC, FL1 and FL2 (DNA staining with propidium iodide (PI)), or alternatively FL3 (DNA staining with DRAQ7). DNA data are collected in pulse height, area and width parameters (FL2-H, FL2-A, FL2-W and FL3-H, FL3-A, FL3-W, respectively), and protein data are collected in height parameters only (FL1-H for Alexa Fluor 488).

Data analysis and calculation (Steps 54–77). Data analysis may be performed with BD CellQuest Pro 6.0 used for data acquisition, but for reasons of convenience we use FlowJo 7.6.5 (Tree Star). FlowJo is a user-optimized software for the high-quality analysis of flow cytometry data regardless of the cytometer used to collect the data. Information on the software fundamentals can be found at http://www.flowjo.com/home/tutorials/ and http://www.flowjo.com/home/manual.html; we recommend quickly going through this information before starting with data analysis. Basics of software handling (e.g., how to create workspaces or analysis plots) can be easily acquired by following these links and are not provided here. Instead, the main procedure of data analysis is brought into focus (**Fig. 3**).

Limitations

The main limitation of this type of assay may be the varying feasibility of cells for biochemical fractionation. Although the included fractionation protocol is widely proven and can be applied to numerous cells of various origins (see MATERIALS and ANTICIPATED RESULTS)[8–11], some cell types may exist that harbor fundamental biochemical differences and for which nuclei cannot be isolated at sufficient quality. Application of protocols based on a different methodology may be an alternative to overcome this limitation. However, even cells entirely refractory to fractionation can be analyzed when constrained to the whole-cell part of the assay, thereby yielding information on the putative cell cycle regulation of a particular protein of interest.

MATERIALS

REAGENTS

- Chang medium C, lyophilized (100 ml; Irvine Scientific, cat. no. T101-019); the kit consists of two components: basal medium (Chang B) and lyophilized supplement (Chang C)
- Minimal essential medium-α (MEM-α; Invitrogen, cat. no. 41061-029)
- Fetal bovine serum, defined (Hyclone, cat. no. HY-ME-SH30070-03)
- L-Glutamine, 200 mM concentrate (PAA, cat. no. M11-004)
- DPBS (short PBS, 1×), without calcium and magnesium (Dulbecco's phosphate-buffered saline; PAA, cat. no. H15-002)
- Trypsin (1:250, Serva, cat. no. 37290)
- EDTA (Sigma-Aldrich, cat. no. E5134)
- Trizma base (Sigma-Aldrich, cat. no. T1503)
- $MgCl_2 \cdot 6H_2O$ (Magnesium chloride hexahydrate, Merck, cat. no. 172571)
- Nonidet P-40 substitute (Sigma-Aldrich, cat. no. 74385)
- HEPES (USB, cat. no. 16926)
- Sodium chloride (NaCl; Sigma-Aldrich, cat. no. S5886)
- Glycerol (Merck, cat. no. 104093)
- Sodium fluoride (NaF; Sigma-Aldrich, cat. no. S7920) **! CAUTION** Sodium fluoride is a general inhibitor of protein phosphoseryl and phosphothreonyl phosphatases and is often used in combination with sodium orthovanadate to preserve protein phosphorylation in cells and cell lysates. It is an inorganic chemical compound and toxic if swallowed. It is irritating to the eyes and skin, and on contact with acids it may liberate a very toxic gas. Avoid contact with skin and eyes and the formation of dust and aerosols. Handle it while wearing gloves, eye shields and a dust mask.
- Sodium orthovanadate (Na_3VO_4; Sigma-Aldrich, S6508) **! CAUTION** Sodium orthovanadate, a general inhibitor of protein phosphotyrosyl phosphatases, is harmful on inhalation, on contact with skin and if swallowed. Avoid contact with skin, eyes and the formation of dust and aerosols. Handle it with gloves.
- DTT solution, 1 M in H_2O (DL-DTT; Sigma-Aldrich, cat. no. 646563)
- Leupeptin trifluoroacetate salt (Sigma-Aldrich, cat. no. L2023)
- Aprotinin (Sigma-Aldrich, cat. no. A1153)
- Benzamidine hydrochloride hydrate (Sigma-Aldrich, cat. no. B6506)
- Trypsin inhibitor (Sigma-Aldrich, cat. no. T9003)
- PMSF (Sigma-Aldrich, cat. no. P7626) **! CAUTION** PMSF is an inhibitor of serine proteases; it is toxic if swallowed and it causes burns. Avoid contact with skin and eyes and the formation of dust and aerosols. Use gloves, eye shields and a dust mask while handling PMSF.
- Paraformaldehyde aqueous solution, 16% (wt/vol), methanol-free, EM (electron microscopy) grade (Electron Microscopy Sciences, cat. no. 15710) **! CAUTION** Paraformaldehyde is used as a fixative, is toxic on inhalation, on contact with skin and if swallowed; it also causes burns. Limited evidence of a carcinogenic effect exists. Handle it while wearing gloves, eye shields and a dust mask. **▲ CRITICAL** For combined protein and DNA staining, we recommend sticking to EM-grade paraformaldehyde at the suggested final concentration. Other concentrations or preparations were shown to have adverse effects on the outcome of the procedure, especially with regard to the quality of DNA staining (**Supplementary Fig. 1**).
- Methanol (Sigma-Aldrich, cat. no. 179957) **! CAUTION** Methanol (also known as methyl alcohol) is highly flammable and is toxic on inhalation, on contact with skin and if swallowed. Avoid contact with skin, eyes and clothing, and handle it with gloves.
- BSA, fraction V (PAA, cat. no. K14-001)
- Primary antibodies for use in flow cytometry (F) and/or immunoblotting applications (IB) (alphabetically listed): α-tubulin–specific antibody, clone DM1A (Calbiochem, cat. no. CP06) (F, IB), β-tubulin–specific antibody, clone 9F3 (Cell Signaling, cat. no. 2128) (F, IB), calnexin-specific antibody, clone 37 (Transduction Laboratories, cat. no. 610523) (F, IB), CENP-A–specific antibody (Cell Signaling, cat. no. 2186) (F, IB), fibrillarin-specific antiblody, clone C13C3 (Cell Signaling, cat. no. 2639) (F, IB), histone H3–specific antibody (Cell Signaling, cat. no. 9715) (F, IB), HSP90-specific antibody, clone 68 (Transduction Laboratories, cat. no. 610418) (F, IB), HSP90-specific antibody (Cell Signaling, cat. no. 4874) (IB), importin α1–specific antibody, alternative karyopherin α2, clone 2 (Transduction Laboratories, cat. no. 610485) (F, IB), jun-specific antibody, clone 3 (Transduction Laboratories, cat. no. 610326) (F, IB), lamin A/C-specific antibody, clone 14 (Transduction Laboratories, cat. no. 612162) (F, IB), lamin A/C-specific antibody, clone 4C11 (Transduction Laboratories, cat. no. 4777) (F, IB), anti-mTOR, clone 7C10 (Cell Signaling, cat. no. 2983) (F, IB), mTOR-specific antibody (Cell Signaling, cat. no. 2972) (F, IB), NUP98-specific antibody, clone C39A3 (Cell Signaling, cat. no. 2598), Oct-3/4–specific antibody (C-10) (Santa Cruz, cat. no. 5279) (F, IB), Oct-3/4–specific antibody (H-134) (Santa Cruz, cat. no. 9081) (F, IB), Oct4A-specific antibody, clone C52G3 (Cell Signaling, cat. no. 2890) (F, IB), p27-specific antibody, clone 57 (Transduction Laboratories, Becton Dickinson, cat. no. 610241) (F, IB), p70S6K-specific antibody, clone 49D7 (Cell Signaling, cat. no. 2708) (F, IB), S6 ribosomal protein–specific antibody, clone 54D2 (Cell Signaling, cat. no. 2317) (F, IB), S6 ribosomal protein S240/244–specific antibody (Cell Signaling, cat. no. 2215) (F, IB), S6 ribosomal protein S240/244–specific antibody, clone D68F8 (Cell Signaling, cat. no. 5364) (F, IB), SOD-2–specific antibody (Stressgen Biotechnologies, cat. no. SOD-110) (F, IB), topoisomerase IIβ–specific antibody, clone 40 (Transduction Laboratories, cat. no. 611492) (F, IB), tuberin/TSC2-specific antibody, clone D93F12 (Cell Signaling, cat. no. 4308) (F, IB) **▲ CRITICAL** This list includes all the antibodies used for experiments presented in the main (**Figs. 2**,**4**–**7**) and supplementary figures (**Supplementary Figs. 1**,**5**–**12**) and may be helpful to the user of this protocol in establishing the assay in the laboratory by recapitulating a particular experiment of interest. With the exception of the HSP90-specific (Cell Signaling, cat. no. 4874) and the SOD-2–specific (Stressgen Biotechnologies, cat. no. SOD-110) antibodies, which have not been tested for use in flow cytometry, all antibodies can be used for both flow cytometry and immunoblotting.
- Species- and subtype-matched control antibodies for use in flow cytometry: rabbit polyclonal isotype control (Santa Cruz, cat. no. sc-3888), rabbit monoclonal isotype control, clone DA1E (Cell Signaling, cat. no. 3900),

mouse monoclonal IgG1 isotype control, clone G3A1 (Cell Signaling, cat. no. 5415), mouse monoclonal IgG2a isotype control (Santa Cruz, cat. no. sc-3878), mouse monoclonal IgG2b isotype control (Santa Cruz, cat. no. sc-3879)
- Secondary antibodies for use in flow cytometry or IBs: goat anti-rabbit IgG (H + L), F(ab)2 fragments, Alexa Fluor 488 conjugate (Cell Signaling, cat. no. 4412), goat anti-mouse IgG (H + L), F(ab)2 fragments, Alexa Fluor 488 conjugate (Cell Signaling, cat. no. 4408), goat anti-rabbit IgG (H + L), HRP conjugate (Bethyl Laboratories, cat. no. A120-101P), goat anti-mouse IgG (H + L), HRP conjugate (Bethyl Laboratories, cat. no. A90-116P)
- PI (Sigma-Aldrich, cat. no. P4170) **! CAUTION** PI is an intercalating fluorescent molecule and is used to stain nucleic acids (DNA and RNA). It is irritating to the eyes, skin and the respiratory system. Avoid contact with skin and eyes and the formation of dust and aerosols. Wear gloves, eye shields and a dust mask while handling PI.
- Trisodium citrate dihydrate (Sigma-Aldrich, cat. no. S1804)
- Ribonuclease A (Sigma-Aldrich, cat. no. R5121)
- Triton X-100 (Sigma-Aldrich, cat. no. X100)
- DRAQ7 (Cell Signaling, cat. no. 7406) **! CAUTION** DRAQ7 belongs to a new generation of DNA dyes and is classified as being toxic. Serious, irreversible effects through swallowing, inhalation and contact with skinmay occur. As for PI, it is recommended to wear suitable protective clothing, gloves and eye/face protection.
- Reagents to run and maintain the flow cytometer: BD FACS flow sheath fluid (Becton Dickinson, cat. no. 342003), BD FACS clean solution (Becton Dickinson, cat. no. 340346), BD FACS rinse solution (Becton Dickinson, cat. no. 340346), BD Calibrite beads (Two-color kit, Becton Dickinson, cat. no. 349502)
- Reagents for standard protein quantification, SDS-PAGE and western blotting for optional immunoblotting experiments[34]
- Roller mixer

EQUIPMENT
- Standard cell culture disposables, including sterile tissue culture plates (e.g., 150 mm × 20 mm, Iwaki, cat. no. 3030-150) and sterile serological pipettes, to grow cells for analysis
- Conical tubes (15 ml, Sarstedt, cat. no. 62.554.502)
- Microcentrifuge tubes (1.5 ml, VWR, cat. no. 2110015)
- Clear, low-retention microcentrifuge tubes for use in antibody stainings (MAXYMum, Axygen, cat. no. AX-MCT-150-L-C)
- Disposable 12 mm × 75 mm (5 ml) polystyrene round-bottom test tubes, capped (FACS tubes) (Becton Dickinson, cat. no. 352054)
- Refrigerated swinging bucket centrifuge with rotor accommodating 15-ml conical tubes (Thermo Fisher, Heraeus Multifuge X3 FR)
- Refrigerated tabletop centrifuge with rotor accommodating 1.5-ml microcentrifuge tubes (Eppendorf, 5417R)
- CASY Cell Counter and Analyzer (Roche, model TTC) or similar equipment (cell counting chamber, hemocytometer) for cell counting
- Inverted phase-contrast microscope achieving magnifications of ×20 and ×40 (combined ocular-objective magnification)
- Standard cell culture equipment (laminar flow hood, humidified tissue culture incubator at 37 °C and 5% CO_2, water bath at 37 °C, fridge and freezer) to grow cells for analysis
- Standard molecular biology equipment (clean single-channel pipettes, 10-, 20-, 200- and 1,000-µl capacity, tips for pipettes, plastic and glassware)
- FACSCalibur benchtop cytometer or similar model equipped with a 488-nm (blue argon) laser for excitation and emission filters for FITC/Alexa Fluor 488 (FL1), PE/PI (FL2) and Cy5-PE/DRAQ7 (FL3); the 635-nm (red diode) laser, optionally available for the Calibur, is not needed as DRAQ 7 can be adequately excited at 488 nm as well
- FlowJo flow cytometry data analysis software (Tree Star, version 7.6.5)
- Equipment for standard protein quantification, SDS-PAGE and western blotting for optional immunoblotting experiments[34]

REAGENT SETUP

Q1 hAFS cells or other cells/cell lines Grow cells in Chang C/MEM-α (1:5) complete growth medium at 37 °C and 5% CO_2 to obtain a 60–80% confluent monolayer. Other cells can be used in the assay, but they have to be tested for their feasibility for biochemical fractionation. The nuclear isolation protocol used here has already been shown to yield reliable results for various cells and may be further adjusted for some others. Tested cells or cell lines include primary human fetal lung fibroblasts (IMR-90)[8,10,11], primary human skin fibroblasts[9], immortalized rodent embryonic fibroblasts (NIH3T3, *TSC2*$^{+/+}$ and *TSC2*$^{-/-}$ MEFs, Rat-1)[8,10,35] and transformed human epithelial cells, e.g., HeLa[35], HEK293 (refs. 35,36) and BxPC-3 cells (see ANTICIPATED RESULTS).

Chang C complete Reconstitute lyophilized Chang C supplement with 10 ml of cell culture–grade H_2O; mix 90% (vol/vol) basic Chang B and 10% (vol/vol) Chang C supplement. It can be stored for up to 6 weeks at 4 °C.

Chang C/MEM-α (1:5) complete growth medium Mix 20% (vol/vol) Chang C complete, 80% (vol/vol) MEM-α, 15% (vol/vol) Hyclone fetal bovine serum and 2 mM L-glutamine. The medium can be stored for up to 6 weeks at 4 °C.

Trypsin-EDTA solution Dissolve 0.4% (wt/vol) trypsin and 0.02% (wt/vol) Na-EDTA in 1× PBS. Filter the solution through a 0.2-µm filter under sterile conditions. Aliquots can be stored at −20 °C for up to 12 months or at 4 °C or at room temperature for several weeks. It can be used for detachment of cells under sterile conditions (routine cell culture), as well as for trypsinization under nonsterile conditions at room temperature (see PROCEDURE).

Extraction buffer A for the isolation of nuclei and the extraction of cytoplasmic proteins Combine 20 mM Tris, pH 7.6, 0.1 mM EDTA, 2 mM $MgCl_2{\cdot}6H_2O$, 0.5 mM NaF and 0.5 mM Na_3VO_4. Store the buffer at 4 °C for several weeks. To yield ready-to-use extraction buffer, supplement protease inhibitors by adding 10 µl of 100× protease inhibitor mix (PIM) and 10 µl of 100× PMSF to 980 µl of extraction buffer A shortly before use.

Extraction buffer B for the (optional) extraction of nuclear proteins Combine 20 mM HEPES (pH 7.9), 400 mM NaCl, 25% (vol/vol) glycerol, 1 mM EDTA, 0.5 mM NaF, 0.5 mM Na_3VO_4 and 0.5 mM DTT. Store the buffer in aliquots at –20 °C for several months. To yield ready-to-use extraction buffer, supplement protease inhibitors by adding 5 µl of 100× PIM and 5 µl of 100× PMSF to 490 µl of extraction buffer B shortly before use.

PIM stock solution (100×) Dissolve 200 µg ml^{-1} aprotinin, 200 µg ml^{-1} leupeptin, 30 µg ml^{-1} benzamidine hydrochloride and 1 mg ml^{-1} trypsin inhibitor in H_2O. Store the solution in aliquots at –20 °C for 6 months. Do not freeze and thaw the solution. PIM is used at a final concentration of 1×.

PMSF stock solution (100×) Prepare a 100 mM solution in isopropanol. Store the solution in aliquots at –20 °C for 6 months. PMSF is used at a final concentration of 1×.

Nonidet P-40 substitute stock solution (10×) Prepare a 10% (vol/vol) solution in H_2O and store it at room temperature for 6 months.

Staining buffer (1×) Dissolve 0.5% (wt/vol) BSA in 1× PBS. Freshly prepare the buffer before use.

PI staining solution (1×) Dissolve 0.025% (wt/vol) PI, 0.005% (wt/vol) RNase, 0.1% (vol/vol) Triton X-100 and 0.1176% (wt/vol) trisodium citrate dihydrate in H_2O. Store the solution in aliquots at –20 °C for 6 months.

DRAQ7 staining solution (1×) Dilute the DRAQ7 stock solution (supplied ready-to-use) 1:500 in 1× PBS to obtain a 3 µM working solution. Freshly prepare the solution before use.

EQUIPMENT SETUP

Flow cytometer checkout Monitor the performance and alignment of the FACSCalibur by standard fluorescent beads (CaliBRITE beads, two-color kit containing unlabeled, FITC-labeled and PE-labeled beads) and the FACSComp software. The beads (polymethylmethacrylate microspheres of ~6 µm) are used to adjust instrument settings, set fluorescence compensation and check instrument sensitivity. Briefly, prepare one tube of unlabeled beads and one tube of mixed (unlabeled + FITC + PE) beads. Enter their lot numbers in the 'Set Up' display. Run the unlabeled beads first and initiate the automatic adjustment of photomultiplier tubes. Remove the sample and insert the bead mixture. Start the automatic fluorescence compensation adjustment and finally perform the sensitivity test. An instrument-settings file with updated FACSComp settings is stored as a Calib file. See also http://www.bdbiosciences.com/documents/BD_FACSCalibur_instructions.pdf.

PROCEDURE

Detachment and preparation of adherent cells for fractionation ● TIMING ~15 min

1| Use a 60–80% confluent monolayer of cells. With respect to Q1 hAFS cells, this corresponds to about 5.0 × 10^6 cells per 15-cm dish. As the subsequent staining of a minimum of 2.0 × 10^5 whole cells or isolated nuclei per condition gives adequate results, one such plate is sufficient to perform flow cytometric analyses of up to four different target proteins in whole cells and isolated nuclei, including the loss of material during nuclear isolation and including all necessary controls.
▲ **CRITICAL STEP** For estimating the amount of starting material (cell number, number of plates), it is important to include the loss of nuclei during purification. The rate of nuclear recovery for Q1 cells is 70–80%. When you are using cells different from the ones described here, it is recommended to verify the overall recovery in a preliminary experiment before performing the whole procedure. However, a good starting point is the initial use of 2.0–5.0 × 10^6 cells in total.

2| Aspirate the medium and briefly rinse the monolayer with 10 ml of ice-cold 1× PBS. The aspirated medium can be collected, stored at 4 °C and reused in later experiments to inactivate the trypsin after trypsinization has been completed (see Step 5).

3| Aspirate PBS and directly add 1 ml of the 0.4% (wt/vol) trypsin-EDTA room-temperature solution. Disperse the solution by gently rotating the plate back and forth and incubate it on the benchtop for 1–3 min at room temperature. Alternatively, the plates can be incubated on an orbital shaker.
▲ **CRITICAL STEP** It is important not to markedly exceed the suggested incubation times, as this increases the risk of cell clumping and premature cell lysis. Q1 hAFS cells have a more fibroblast-like morphology (**Fig. 1b**); they grow in a single-cell manner and can be very efficiently trypsinized. For other cells, incubation times may need to be adjusted, but we have never observed times exceeding 3 min. Alternatively, the trypsin-EDTA solution can be preincubated at 37 °C shortly before use to speed up the reaction. Furthermore, it is essential to ensure a certain degree of plate-to-plate consistency during the harvesting procedure, as the analysis of cell size in general is very sensitive. If multiple plates are handled simultaneously, we recommend storing monolayers in PBS on ice until they are ready for trypsinization. Stacks of no more than five plates should be handled at once. Upon preparation, the trypsin solution is frozen in aliquots of 10 ml and stored at −20 °C. After initial use, the remaining trypsin can be stored at room temperature for up to several weeks without substantial loss of enzymatic activity.

4| Gently tap the plate until cells detach. Detaching cells can be easily identified without microscopic evaluation, as they come off as white clusters.

5| Immediately add 5 ml of ice-cold, serum-containing growth medium to inactivate the trypsin. Disperse trypsinized cells in medium by gently resuspending them three or four times to produce a single-cell suspension.
▲ **CRITICAL STEP** Having the monolayer dispersed as single cells is very important, as the subsequent steps of fixation and permeabilization tend to aggregate cells *per se*. During flow cytometric acquisition, these aggregated cells are omitted, thus limiting the amount of cells that can be efficiently used for data analysis.
? TROUBLESHOOTING

6| Transfer the suspension to a 15-ml conical tube and pellet the cells by centrifugation at 200*g* (~1,000 r.p.m.) for 2 min at 4 °C.

7| Discard the supernatant and resuspend the pellet in 1 ml of ice-cold 1× PBS. Put the cells on ice and use a small aliquot to estimate the number of viable cells using a CASY cell counter and analyzer or similar equipment.

8| Pellet cells by centrifugation at 200*g* for 2 min at 4 °C and discard the supernatant. This corresponds to a simple washing step to eliminate residual traces of fetal calf serum from the trypsin inactivation step.
▲ **CRITICAL STEP** If only flow cytometric analyses are performed, this washing step can be omitted to reduce hands-on time. In some cases, however, it may be interesting and/or important to evaluate both flow cytometry and immunoblotting in parallel. For subsequent cell or nuclei lysis, it is essential to remove traces of serum and growth medium, as their presence may interfere with the immunodetection step of the immunoblotting approach.

9| Resuspend the pellet in 1 ml of ice-cold 1× PBS.

10| Transfer around one-third of the cell suspension (330 µl containing ~1.7 × 10^6 cells) to a new 15-ml conical tube. Pellet the cells in a final centrifugation step at 200*g* for 5 min at 4 °C and dilute the suspension with ice-cold 1× PBS to a final

concentration of 0.5 × 10^6 cells per ml (~3.4 ml of 1× PBS). Put the cells on ice. These cells, constituting the population of whole cells, are omitted from the fractionation procedure and are further processed for fixation and permeabilization.
■ **PAUSE POINT** Short-term storage (15–20 min) of (whole) cells in PBS was found to be neither associated with reduced cell viability and integrity nor with perturbations in protein expression or phosphorylation (e.g., intracellular redistribution of proteins) when compared with continuously processed cells. Although cells in PBS may thus be stored on ice until the nuclear isolation of the remaining cells has been completed, it is recommended to directly continue with fixation and permeabilization steps (Steps 25–31).

11| Transfer the remaining cells (about two-thirds of the cell suspension or 660 µl containing ~3.4 × 10^6 cells) in a 1.5-ml microcentrifuge tube and pellet the cells in a final centrifugation step at 200*g* for 5 min at 4 °C. This ratio of 1:3 in splitting the initial pool of cells for further processing (one part of cells to be used for whole-cell processing and two parts to be used for isolation of cell nuclei) has proven to be reliable and includes the potential loss of material during sample preparation. For data analysis and calculation, it is essential that the fractions to be compared, whole cells versus isolated nuclei, originate from the same pool of cells processed under identical conditions.

12| Thoroughly discard the supernatant and put the cells on ice.

Isolation of pure, intact nuclei via biochemical fractionation ● TIMING ~25–30 min
13| Resuspend the cell pellet from Step 12 (with a pellet volume of about 50 µl) in five pellet volumes (~250 µl) of extraction buffer A (cytoplasmic extraction buffer). Carefully pipette the mixture up and down using a 1-ml tip to obtain a single-cell solution. Owing to the relatively high amount of cells, the suspension looks slightly yellowish.
▲ **CRITICAL STEP** The amount of extraction buffer used is a crucial and rate-limiting parameter for the yield and purity of isolated nuclei. If too little extraction buffer is used, this may result in insufficient cell lysis, causing severe contamination of nuclear pellets. Five pellet volumes of extraction buffer are a reliable condition to start with, but more could be used at the user's discretion. The maximum amount, however, should not exceed ten pellet volumes, as this leads to excessive dilution of the cytoplasmic extract, which may be coanalyzed in parallel.

14| Incubate the cells for 2 min at room temperature and for another 10 min on ice to induce hypotonic swelling of cells as a preparative step for subsequent cell lysis.

15| Add 25 µl of a 10% (vol/vol) solution of Nonidet P-40 substitute to obtain a final concentration of 1% and mix it by gently vortexing or inverting the tube. This induces cell membrane disruption and the release of cytoplasmic proteins while keeping nuclear membranes intact.

16| Homogenize broken cells by gently pipetting up and down three times using a 200-µl tip or a 20-G needle.
▲ **CRITICAL STEP** The introduction of air bubbles during this step should be largely avoided, as this leads to substantially reduced nuclear yield.

17| Separate the cytoplasmic extract from intact nuclei by low-speed centrifugation in a prechilled tabletop centrifuge at 4 °C and 500*g* for 3 min. The nuclear pellet looks brightly white and less dense when compared with a pellet of intact, whole cells.

18| Aspirate ~80% of the supernatant and transfer it to a new 1.5-ml microcentrifuge tube (C, cytoplasmic extract). Discard the residual 20% thoroughly. The pellet contains nuclei of low purity contaminated with unbroken or insufficiently lysed cells and nonsoluble parts of the cell membrane. This approach for creating a cytoplasmic extract is recommended to avoid carryover of intact, slightly damaged or leaky nuclei to the cytoplasmic fraction and to minimize loss of nuclei due to accidental aspiration of the pellet. Store the tube containing the fraction of soluble cytoplasmic proteins at –80 °C for optional use in immunoblot analyses.

19| Directly add Nonidet P-40 substitute to 1 ml of extraction buffer A to a final concentration of 1% (vol/vol). Mix the tube by vortexing. Add 10–15 pellet volumes (200–300 µl) to the pellet of crude nuclei.

20| Gently resuspend the nuclei by pipetting up and down using a 200-µl or 1,000-µl tip to wash and further purify the crude nuclear preparation.

21| Pellet the nuclei by centrifugation at 4 °C and 500*g* for 3 min and roughly discard the supernatant.

22| Repeat this washing step (Steps 19–21) once.
▲ **CRITICAL STEP** During these washing steps, the nuclear pellet is typically getting smaller, with an average loss of about 10–20% of the original pellet. This is most likely due to the lysis of unbroken cells that escaped the procedure during the cytoplasmic extraction step. In contrast, it is difficult to avoid breaking some nuclei during the purification step, causing the release of genomic DNA. This makes the pellet of nuclei slightly viscous when compared with a pellet of whole, intact cells. Slightly forced pipetting is thus necessary to resuspend nuclei. Minor aggregation of isolated nuclei is encountered, can be hardly evaded and contributes to some extent to the loss of material for flow cytometric analysis. However, increased loss of the nuclear pellet volume indicates excessive nuclear breakage. This occurs if the amount of detergent in extraction buffer A is too high (dependent on cell type), if too many washing steps are performed or if incubation between centrifugation steps is prolonged. The sensitivity of nuclear integrity with respect to the amount and type of detergent can markedly vary between cell lines and must be thoroughly tested.
? TROUBLESHOOTING

23| Resuspend purified nuclei in ~200 µl of extraction buffer A containing 1% (vol/vol) Nonidet P-40 substitute. During this final washing step, the overall quality of the nuclear preparation can be roughly estimated either microscopically (**Fig. 1b**) or by means of cell size analyses using a CASY cell counter and analyzer or similar equipment (**Fig. 1c**).

24| At this stage of the protocol, it is optional and convenient to use an aliquot of the preparation to extract soluble nuclear proteins that can be separately analyzed via immunoblotting (**Fig. 2**). Extraction of soluble nuclear proteins is briefly described under option A. Completing the workup of the purified nuclei is described in option B.

(A) Extraction of soluble nuclear proteins

(i) Transfer 100 µl of the purified nuclei (Step 23) to a new 1.5-ml microcentrifuge tube; spin down the tube at 4 °C and 500*g* for 3 min and carefully discard the supernatant. This 100 µl of purified nuclei is not included in the initial calculation of the overall amount of staring material (Step 1) and will reduce the number of possible flow cytometric analyses from four to two different proteins. In the case of Q1 hAFS cells, the nuclear extraction using a total of around 1.7×10^6 isolated nuclei typically yields 50–80 µg protein, which is sufficient to perform multiple immunoblotting experiments by following standard procedures for SDS-PAGE and western blotting. For anticipated results see **Figure 2a**,**b** (Detailed information on the used cell synchronization and immunoblotting procedure can be found elsewhere[10,34].).

(ii) Resuspend the nuclear pellet in one to two pellet volumes (~20–30 µl) of extraction buffer B (nuclear extraction buffer) and vortex it vigorously.

(iii) Snap-freeze the mixture twice in liquid nitrogen and incubate it for 20 min on ice.

(iv) Separate soluble nuclear proteins from the nonsoluble fraction by high-speed centrifugation at 4 °C and 20,000*g* for 20 min.

(v) Collect the supernatant (N, soluble nuclear proteins) and store it for up to 12 months at –80 °C.

(B) Last stages of workup of purified nuclei

(i) Pellet the nuclei by centrifugation at 4 °C and 500*g* for 3 min and thoroughly discard the supernatant. Put the nuclei on ice.

(ii) Resuspend the nuclei in 200 µl of ice-cold 1× PBS and use a small aliquot to estimate the nuclei number. The expected yield is about 2.4×10^6 nuclei, considering the anticipated loss of material during preparation. Keep the tubes on ice.
? TROUBLESHOOTING

(iii) Transfer the suspension to a 15-ml conical tube and bring it to a final concentration of 0.5×10^6 nuclei per ml by diluting it with ice-cold 1× PBS (~4.8 ml).

Fixation and permeabilization of whole cells and isolated nuclei ● TIMING ~20 min
▲ **CRITICAL** Whole cells (Step 10) and isolated nuclei (Step 24B(iii)) are processed separately (in separate tubes), but under identical conditions.

25| Directly add methanol-free, 16% (wt/vol) room-temperature paraformaldehyde to whole cells and isolated nuclei in PBS to obtain a final concentration of 1.5% (vol/vol) paraformaldehyde (~320 µl for whole cells and ~550 µl for isolated nuclei).
▲ **CRITICAL STEP** For combined protein and DNA staining, we recommend sticking to EM-grade paraformaldehyde at the suggested final concentration. Other concentrations or preparations have been shown to have adverse effects on the outcome of the procedure, especially with regard to the quality of DNA staining (**Supplementary Fig. 1**).
? TROUBLESHOOTING

26| Fix the samples while incubating them on a roller mixer for 10 min at room temperature under constant, mild agitation (~25–30 r.p.m.).

▲ CRITICAL STEP Predilution of whole cells and isolated nuclei in PBS (Steps 10 and 24B(iii)) and incubation under constant rotation (Step 26) decrease the likelihood of aggregation during fixation. It is thus recommended to stick to this procedure in order to avoid irreversible aggregation and thus loss of material for analysis.

27| Collect cells and nuclei by centrifugation at 4 °C and 500*g* for 5 min in a swinging-bucket rotor. At this stage, whole cells and isolated nuclei can be clearly discriminated, as pellets of fixed, whole cells are compact, brightly white and well defined, whereas pellets of fixed nuclei appear sheer white and are poorly visible.
▲ CRITICAL STEP Do not use a centrifugal force less than 500*g*, as it leads to insufficient pelleting and loss of fixed nuclei.
? TROUBLESHOOTING

28| Decant the supernatant by gently inverting the tubes, leaving the pellet of cells or nuclei at the bottom.

29| Resuspend the pellets in residual PBS/paraformaldehyde (typically 50–150 µl) by first vigorously flicking the tube, then pipetting up and down twice using a 200-µl tip and finally briefly vortexing it for 3–5 s. Place the tubes on ice.

30| Permeabilize cells or nuclei by slowly adding cold (−20 °C) 100% methanol to prechilled samples, while gently vortexing, to obtain a final concentration of ~0.5 × 10^6 cells or nuclei per ml 100% methanol (~3.4 ml of methanol for whole cells and ~4.8 ml for isolated nuclei).

31| Place the tubes on ice for 15–30 min.
■ PAUSE POINT At this stage of the protocol, samples can be stored at −20 °C for at least 3 weeks without any adverse effects on the outcome of the procedure. For prolonged storage, samples may be kept at −80 °C.

Protein and DNA staining of whole cells and isolated nuclei ● TIMING **~2.5 h**
▲ CRITICAL The following steps are carried out at room temperature.

32| Aliquot 2.0 × 10^5 cells or nuclei per condition (~400 µl) into a 1.5-ml microcentrifuge tube.
▲ CRITICAL STEP This protocol was adjusted to use a minimum of cells or nuclei to obtain reliable results. Because pellets of 2.0 × 10^5 cells or nuclei are small and the nuclear pellet is rather hard to identify (see Step 27), it is recommended to use clear, low-retention tubes during the staining procedure to avoid loss of material.

33| Add 1 ml of staining buffer and mix it by inverting the tubes two or three times.
▲ CRITICAL STEP Do not mix the sample by pipetting, as this leads to loss of material. The staining buffer should be freshly prepared every day.

34| Pellet cells or nuclei by centrifugation at 500*g* for 3 min in a swinging-bucket rotor.

35| Roughly discard the supernatant using a 1,000-µl tip and thoroughly remove the residual staining buffer with a 200-µl tip.

36| Resuspend the pellet in 100 µl of staining buffer.

37| Incubate the mixture for 10 min at room temperature. This corresponds to a short blocking step.

38| Add 10 ng of the unconjugated primary antibody (or 10 ng of the species- and subtype-matched control antibody for use as a negative control) to the tubes and mix by gentle vortexing.
▲ CRITICAL STEP The right amount of primary antibody was shown to be essential in order to obtain specific staining results (**Supplementary Fig. 5a–d**). Depending on the overall quality and specificity of the antibody, excessive amounts can cause intense background staining, which spuriously gives a strong, positive signal even when compared with the same amounts of isotype control (**Supplementary Fig. 5a**). A final amount of 50 ng antibody per 1 × 10^6 cells yielded the best results for most of the tested antibodies, but further optimization might be necessary or beneficial for your chosen antibody. It is worth noting that, in terms of specificity, we obtained best results with monoclonal antibodies of either mouse or rabbit, whereas polyclonals were more likely to require careful optimization. Moreover, it is crucial to keep the volume of staining buffer constant between samples and experiments, as this influences the staining efficiency. Depending on the antibody concentration, typically 0.2–2.0 µl of the primary antibody is used; the total volume of the staining reaction should not exceed 120 µl.

39| Incubate the sample for 60 min at room temperature. For many antibodies, the incubation time may be reduced to 30 min without any adverse effects on the staining efficiency, but this has to be carefully tested.
■ **PAUSE POINT** At this stage of the protocol, the 1-h incubation at room temperature may be exchanged for overnight (~12–16 h) incubation at 4 °C. However, when comparing multiple, independent experiments using one particular antibody, we recommend sticking to the same standard procedure.

40| Add 1 ml of staining buffer and mix it by inverting the tubes two or three times. Again, do not resuspend pellets. This corresponds to a washing step to remove free, unbound antibody.

41| Pellet cells or nuclei by centrifugation at 500*g* for 3 min in a swinging-bucket rotor and discard the supernatant as described in Step 35.

42| Resuspend the pellet in 100 µl of staining buffer.

43| Add the fluorochrome-conjugated secondary antibody at a dilution of 1:500 and incubate it for 30 min at room temperature. Incubation in the dark (or by covering the tube rack) can be performed, but it was found to be without any benefit when compared with staining on the benchtop. To establish this protocol, we used Alexa Fluor 488 conjugates, with excitation and emission properties nearly identical to those of FITC, almost exclusively. Compared with FITC, Alexa Fluor 488 tends to be brighter and better for intracellular applications including standard fluorescence microscopy, which can be used to reexamine and reevaluate stained samples after acquisition and analysis on the flow cytometer. Moreover, these conjugates can be very efficiently combined with fluorescent DNA dyes with an emission color in the orange (PI) and far-red (DRAQ7) spectra.

44| Repeat Steps 40 and 41.
? TROUBLESHOOTING

45| Counterstaining of DNA can be performed using two different options, depending on whether the user is less or more experienced in setting up the cytometer, especially with respect to the compensation for partially overlapping emission spectra of different fluorochromes. Option A involves counterstaining with PI, and analysis requires compensation. Option B uses DRAQ7 staining, and analysis does not involve compensation. DRAQ7 is a far-red fluorescent dye that, similarly to PI, only stains the DNA of dead and permeabilized cells or nuclei. However, as it is DNA specific, no concomitant RNase treatment is required. It can be excited at multiple wavelengths (including 488-nm lasers used for PI excitation), but it has more convenient spectral properties in that no emission overlap with FITC/Alexa Fluor 488 is observed.

(A) Counterstaining with PI, compensation required

(i) Carefully resuspend cells or nuclei in 300–400 µl of PI staining solution.

(ii) Incubate the samples for 20 min on ice and transfer them to 5-ml capped, round-bottom test tubes. Directly proceed to sample acquisition on the flow cytometer. Alternatively, if samples are to be stored before acquisition (see the **PAUSE POINT** below), centrifuge them at 500*g* for 3 min and resuspend them in 300–400 µl of 1× room-temperature PBS.
▲ **CRITICAL STEP** PI is a nucleic acid stain that binds to both DNA and RNA. Hence, removal of RNA by RNase treatment of samples is necessary. An appropriate amount of DNase-free RNase is included in the PI staining solution and efficiently removes RNA by incubation on ice. Insufficient removal can be recognized by a significant broadening of G1 and G2 peaks, which complicates proper gate setting for discrimination of cell cycle subsets. Moreover, DNA staining can be easily verified under the microscope to exclude nonspecific or RNA-specific staining of the cytoplasm. Properly stained cells exclusively show nuclear fluorescence, even when pictures are overexposed (**Supplementary Fig. 1b**). Combination of Alexa Fluor 488 conjugates and PI requires compensation in both directions, with only minor adjustments to compensate for the overspill of PI emission in the green (Alexa Fluor 488) spectrum. For more detailed information on instrument settings, see later stages of the protocol (Steps 48–51).

(B) Counterstaining with DRAQ7, no compensation required

(i) Ready-to-use DRAQ7 is supplied as a 0.3 mM stock. Prepare an appropriate amount of a 1:100 dilution of DRAQ7 in 1× PBS to obtain a final concentration of 3 µM.

(ii) Carefully resuspend the cells or nuclei in 300–400 µl of DRAQ7 staining solution and transfer them to 5-ml capped, round-bottom test tubes.

(iii) Incubate the suspension for 10 min on ice. Staining is known to be accelerated at 37 °C, and thus incubation times may be reduced; however, this has to be thoroughly tested. Cells or nuclei can be directly analyzed or stored in the presence of DRAQ7; washing or removal of the dye is not required.

■ **PAUSE POINT** At this point of the protocol (options A and B), it is possible to store double-stained cells or nuclei for at least 12–16 h (overnight) at 4 °C before acquisition on the flow cytometer. Although we observed no major loss of signal strength (data not shown), we recommend sticking to a standard procedure and ensuring day-to-day consistency in the timing of sample acquisition to avoid interassay variability in results.

Data acquisition on the flow cytometer ● TIMING ~1 h

46| Start up the flow cytometer and the computer, perform the usual fluidics maintenance and launch CellQuest Pro.

47| Open the appropriate acquisition document from the storage folder or, alternatively, create a new one. This document is suggested to include dot plots of FSC versus SSC (overall definition of the cell population and rough live/dead discrimination), FL2 (or 3)-W versus FL2 (or 3)-A (DNA doublet discrimination), FL2 (or 3)-A versus FL1-H (protein expression in relation to DNA content) and FSC versus FL1-H (protein expression in relation to cell size), as well as histogram plots of FSC, FL1-H and FL2 (or 3)-A.

48| Connect to the cytometer and launch or create appropriate instrument settings. For Q1 whole cells and nuclei that are counterstained with DRAQ7 and excited at 488 nm, initial cytometer settings are used: FSC (voltage E-1, ampgain 6.42–6.72, linear mode), SSC (voltage 198, ampgain 1.00, logarithmic mode), FL1 (voltage 390-436, ampgain 1.00, logarithmic mode), FL3 (voltage 574-569, ampgain 1.00, linear mode), FL3-A (ampgain 1.18, linear mode), FL3-W (ampgain 5.08, linear mode), primary threshold parameter: FSC, value 20; secondary threshold parameter: FL3, value 20.
▲ **CRITICAL STEP** These settings represent a reference or starting point to roughly define the cell population (whole cells and nuclei) with respect to size, DNA and specific protein content. Further adjustment of detector gains and voltages may be necessary.

49| Adjust the FSC detector. When starting up the setting with whole cells, it should be kept in mind that the amplification gain for the FSC detector has to be adjusted at higher levels so that isolated nuclei can be acquired and displayed under identical conditions. Depending on the cell type–specific relation of total cell size toward nuclear size, whole cells can be clearly separated cytofluorometrically from isolated nuclei, with the latter showing substantially lower FSC and SSC intensities (**Fig. 4**).

50| Adjust the FL2 (or 3) gain. Whole cells and isolated nuclei have the same DNA content and thus show almost identical FL2 (or 3) signal strength. Some minor differences are observed in that nuclei tend to have slightly more DNA-specific fluorescence, which is identically distributed between cell cycle phases when compared with whole cells. We assume this to be due to a better staining efficiency of isolated nuclei through removal of the cell membrane, and to some extent, to components of the cytoplasm, which may contribute to some retention of the dye. Therefore, the FL2 (or 3) gain has to be slightly adjusted between populations, with the G1 peaks of both being set to a value of around 200. This enables direct comparison of DNA-specific signals at the same resolution and allows copying and pasting gates for cell cycle discrimination of whole cells and isolated nuclei.

51| Adjust the FL1 gain. The FL1 gain, in contrast, is kept constant between measurements of whole cells and nuclei to account for slight variations in signal strength. Although mouse monoclonal control antibodies bound to nuclei show a weaker signal when compared with whole cells, rabbit monoclonal control antibodies yield very similar results when bound to nuclei or whole cells. These differences in the background staining between whole cells and isolated nuclei are considered in the later steps of data calculations (Step 71).
▲ **CRITICAL STEP** If PI is used instead of DRAQ7, compensation is required. As a certain amount of Alexa 488 fluorescence (depending on the overall signal strength) is collected by the FL2 detector and a small amount of PI fluorescence is collected by the FL1 detector, electronic subtraction (compensation) must be performed to avoid false positive results. Typical compensation settings are FL1—0.1% FL2 and FL2—35.0% FL1; FL2 (voltage 320–350, ampgain 1.00, linear mode), FL2-A (ampgain 1.18, linear mode), FL2-W (ampgain 5.08, linear mode).

52| Collect a total of 1.0×10^4 to 5×10^4 cells or nuclei per sample at medium flow rate. The plot for doublet discrimination is used to set acquisition and storage gates. As nuclei are more prone to aggregation than whole cells, an average loss of 20–30% will be encountered. Acquisition of nuclei therefore takes longer.

53| After completing data acquisition and storage, perform the usual fluidics maintenance and proceed to data analysis.

Data analysis and calculation ● TIMING ~3–5 h

54| Launch FlowJo on your computer and import data files in flow cytometry standard format (.fcs file extension) into a new workspace.

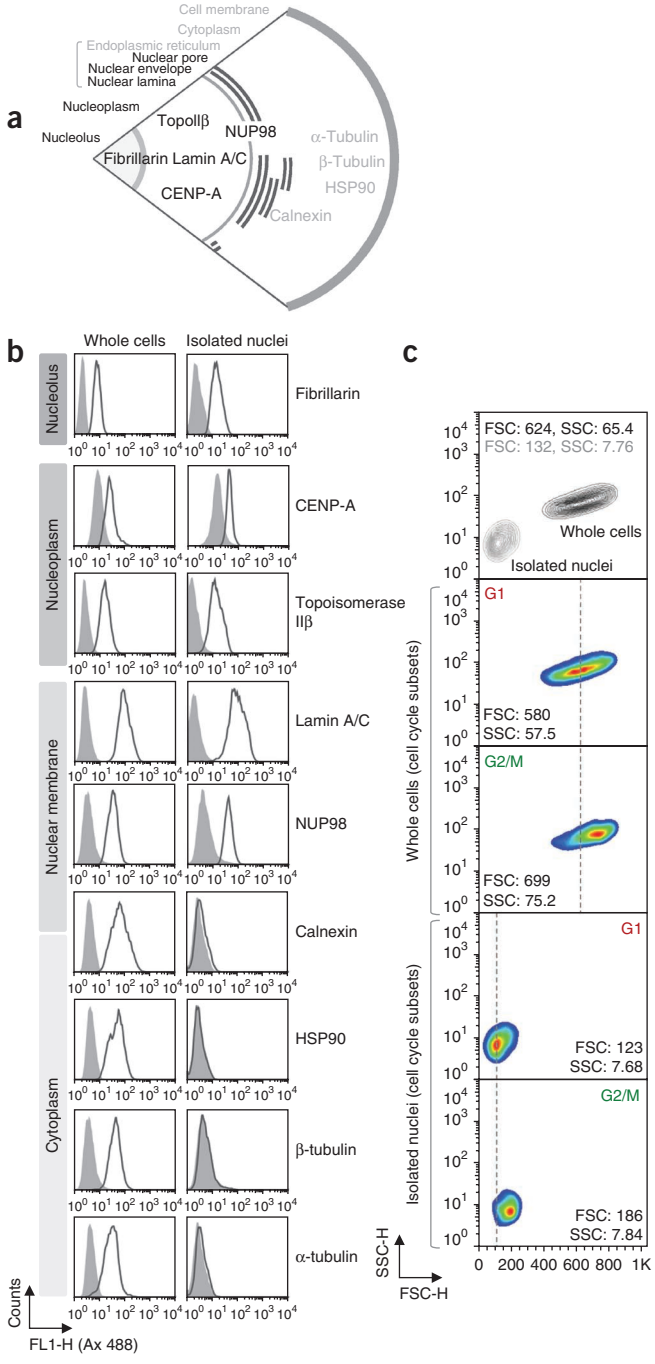

Figure 4 | Flow cytometric characterization of isolated nuclei. (**a**) Illustration of subcellular layers and marker proteins analyzed in this study. (**b**) Flow cytometric analyses of Q1 whole cells and isolated nuclei labeled for the indicated subcellular marker proteins. Corresponding histograms are presented (filled curves, control IgGs; open curves, specific IgGs). (**c**) Two-dimensional contour (top) and density (adjacent) plots comparing forward (FSC-H)-scatter and side (SSC-H)-scatter properties of Q1 whole cells versus isolated nuclei. Plots are either shown for whole populations (top image) or their corresponding G1 and G2/M subsets (lower images). A dotted gray line was set into the center of the G1 populations to visualize the shift in the G2/M populations. Median FSC-H and SSC-H values are included. Ax 488, Alexa Fluor 488.

55| Perform DNA content–based doublet discrimination using a bivariate plot of FL2 (or 3)-W versus FL2 (or 3)-A. Include all samples, whole cells and isolated nuclei, stained with either the specific or the control antibody. Exclude aggregates or doublets (at high FL2-W values), debris (at low FL2-W and low FL2-A, <200, values) and the diploid continuum (at high FL2-A values, >400) to yield populations of single, intact cells or nuclei.

▲ **CRITICAL STEP** Prior FSC and SSC discrimination of dead cells (or cell debris) and intact cells, as usually performed to roughly define the population of interest, is not done. Although this works fine for whole cells, this approach is not recommended for isolated nuclei: owing to the small size (and the narrow size distribution) of nuclei and the low flow cytometric resolution when compared with whole cells, cell debris and damaged nuclei cannot be reliably separated. In contrast, nuclei tend to aggregate, with multiple (up to 15) nuclei sticking together. This leads to a marked broadening of the population toward an increased FSC. Taken together, this makes reasonable FSC/SSC gating unlikely. Therefore, to use identical conditions for both whole cells and isolated nuclei, prior definition of populations is solely performed on the basis of doublet discrimination via DNA content.

56| Create histogram overlays of cells and nuclei stained with specific antibodies and the corresponding isotype controls.

57| Discriminate between positive and negative signals. A negative staining is defined by almost exactly overlapping curves obtained for the specific and the control antibody, with 100% of cells being negative for the protein of interest (e.g., tubulin, HSP90 and calnexin stainings of isolated nuclei; **Fig. 4**). Partially negative populations are identified as bimodal distributions (two peaks), with a certain percentage of cells being found in the same (negative) area as the isotype control while the remaining cells show a clearly distinguishable, positive signal over the control population (e.g., tuberin staining of *TSC2*$^{+/+}$ MEFs spiked with *TSC2*$^{-/-}$ MEFs; **Supplementary Fig. 5d**). Unimodal distributions (one peak) at similar frequencies (counts) but with increased signal strength when compared with the control-stained populations are classified as containing 100% positive cells, including strongly positive signals (e.g., p27 staining of *TSC2*$^{+/+}$ MEFs under growth condition C, **Fig. 5**, and lamin A/C staining of whole cells, **Fig. 6**), signals of intermediate intensity (e.g., HSP90 staining of whole cells, **Fig. 6**) and weakly positive signals (e.g., mTOR staining of isolated nuclei, **Fig. 6**). With respect to positive signals, bimodal distributions (e.g., p27 staining of *TSC2*$^{+/+}$ MEFs grown under condition C, **Fig. 5**) and asymmetric, unimodal distributions (skewed toward a particular direction) indicate a population in which not all cells uniformly express similar amounts of the protein of interest. This may hint at nonconstitutive (e.g., cell cycle–dependent) protein expression, with different cells within a population (e.g., G1, S and G2/M phase cells) harboring different amounts of a particular protein.

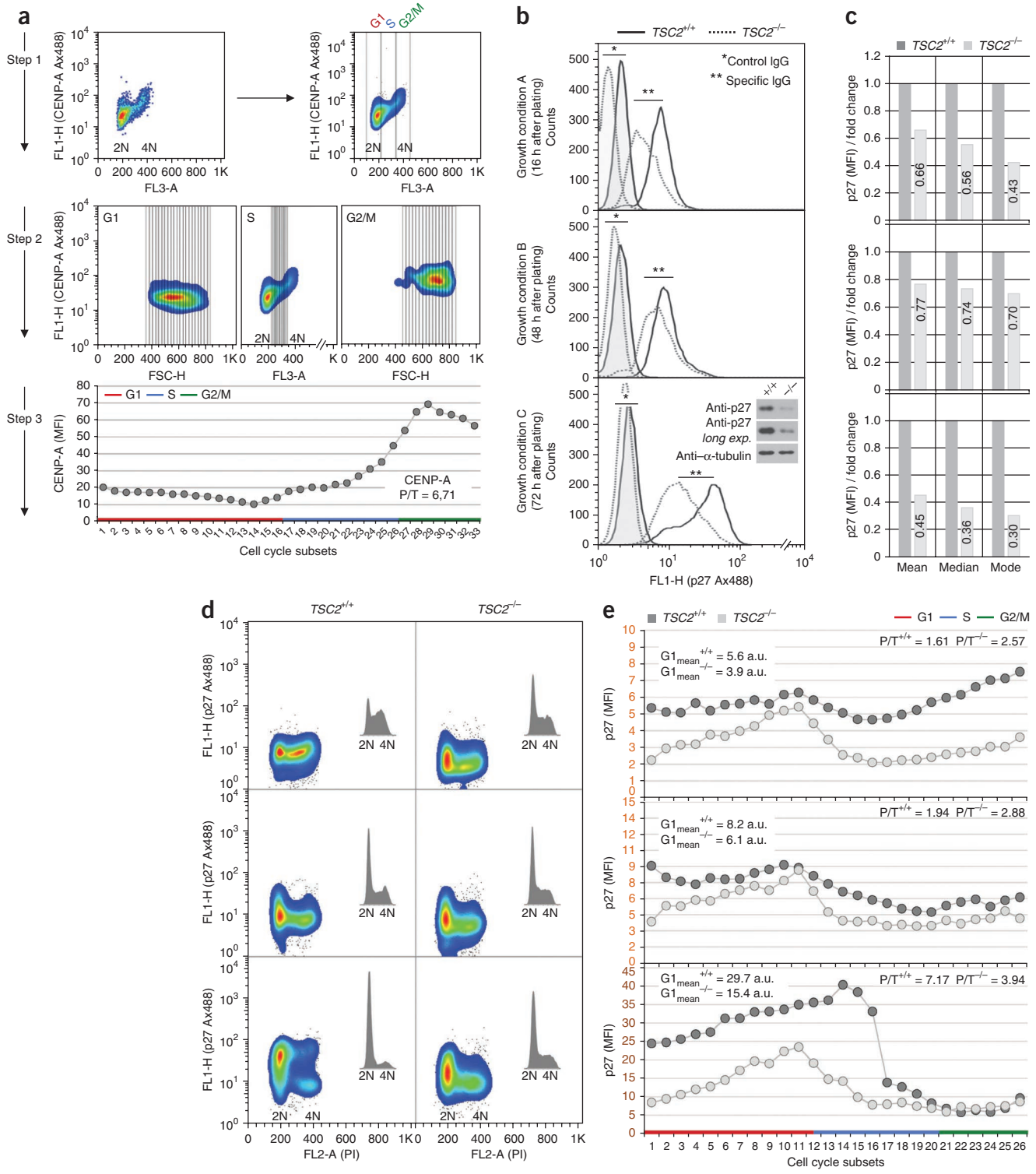

Figure 5 | Monitoring protein expression during the cell cycle via flow cytometry. (**a**) Implementation of the stepwise gating procedure (**Fig. 3**) for the investigation of the CENP-A cell cycle regulation in Q1 hAFS cells. Top (step 1), left: Bivariate density plot of Q1 cells immunostained for CENP-A (FL1-H) and labeled for DNA (FL3-A). Right, smoothed version of the same plot enabling concise positioning of gates to separate G1 (2N), S and G2/M (4N) subsets. Middle (step 2), bivariate density plots showing the cell size– and DNA-specific signal dissection of G1,G2/M and S subsets, respectively, using a rectangular gating tool. Bottom (step 3), contiguous depiction of dissected cell cycle subsets and their corresponding CENP-A median fluorescence intensities (MFIs) in arbitrary units. The P/T ratio is indicated. (**b**–**d**) Cell cycle–dependent expression of p27 in *TSC2*$^{+/+}$ versus *TSC2*$^{-/-}$ MEFs under various growth conditions (conditions A–C). (**b**) histogram overlays of wild-type and knockout MEFs either labeled with antibodies specifically targeting p27 (specific IgG, open curves) or incubated with species- and subtype-matched control immunoglobulins (control IgG, tinted curves). A representative p27 immunoblot analysis of condition C cells is included. (**c**) Depiction of p27-specific mean, median and mode (peak) fluorescence intensities, with values for wild-type MEFs being set to 1.0. (**d**) Bivariate density plots of MEFs stained for DNA (FL2-A) and p27 (FL1-H). Corresponding DNA histograms are included. (**e**) Cell cycle graphs displaying the median p27 fluorescence according to consecutive cell cycle subsets obtained via the stepwise procedure described in **a**. Information on the average fluorescence intensity of G1 phase cells ($G1_{mean}$) is included. P/T ratios are indicated. a.u., arbitrary units.

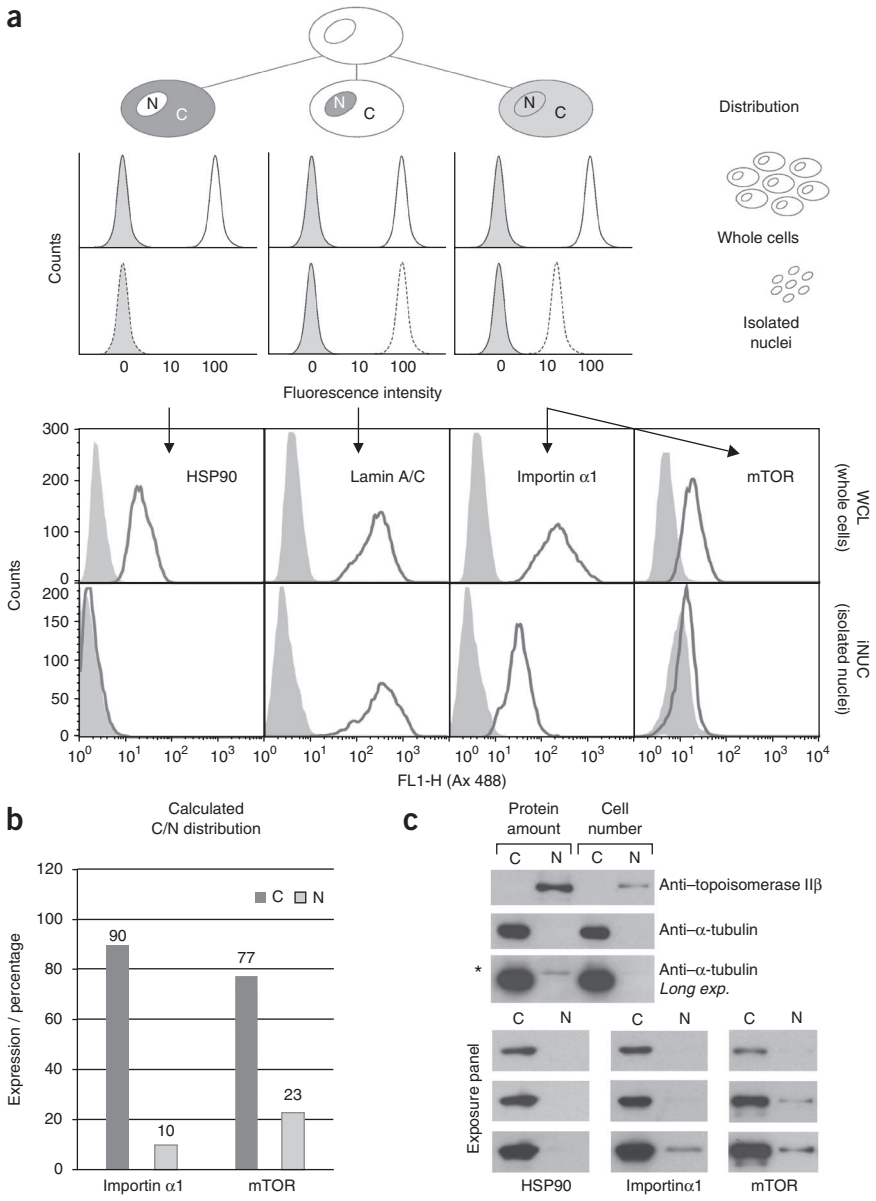

Figure 6 | Monitoring nucleocytoplasmic protein expression via flow cytometry. (**a**) Evaluation of subcellular distribution on the basis of the flow cytometric analyses of whole cells versus isolated nuclei. Illustrated are the three main categories of anticipated results, including exclusive and mixed localization patterns (top); shown are the actual flow cytometric results obtained for marker proteins HSP90 (cytoplasmic), lamin A/C (nuclear), importin α1 and mTOR (both cytoplasmic and nuclear). Filled curves, control IgGs; open curves, specific IgGs. (**b**) Nucleocytoplasmic distribution of importin α1 and mTOR obtained via calculation of flow cytometric whole cell versus nucleus results shown in **a**. (**c**) Immunoblotting analyses of the nucleocytoplasmic distribution of indicated proteins. With the exception of the first blot panel (labeled with 'protein amount'), amount of loaded protein for each fraction was normalized to cell numbers. The asterisk indicates a nonspecific band. C, cytoplasm; N, nucleus.

58| As a prerequisite for the next data analysis steps, verify that isolated nuclei are (100%) negative for coanalyzed cytoplasmic marker proteins. Nuclear marker proteins are expected to show very similar patterns in whole cells and isolated nuclei (**Figs. 4** and **6**).
? TROUBLESHOOTING

59| If applicable (Step 57, partially negative populations), gate for positive signals: create a FL2 (or 3)-A versus FL1-H plot and display the isotype control. During the acquisition, this population is adjusted to appear in the low-intensity area (10^0–10^1) of the FL1-H scale. Use the polygonal gating tool to draw a gate encompassing the high-intensity area, excluding the population of control-stained cells. Copy this gate and paste it to a corresponding plot displaying the specifically stained sample. Check gates for proper adjustment and continue analysis with the (positive) cells enclosed in the gate.
▲ **CRITICAL STEP** The G2/M subset of the nonspecifically stained sample shows slightly stronger fluorescent signals than the G1 subset. Use the polygonal (not the rectangular) gating tool to thoroughly draw the gate for these differences.

60| Create a 2D pseudocolor plot of DNA (FL2 or 3-A) versus protein (FL1-H) and display the specifically stained sample of the whole-cell population (**Fig. 5a**). Smooth the plot to facilitate proper gating and set gates for G1, S and G2/M cell cycle subsets using the rectangular gating tool. Start gating for G1, followed by gating for G2, with the intermediate of the population being defined as the gate for the S phase. It is recommended to set gates toward a pure population of G1 and G2/M cells while including G1/S and S/G2 transitions in the S subset (**Fig. 5a**).
▲ **CRITICAL STEP** We have found that gating for cell cycle subsets yields better results when it is directly performed on 2D pseudocolor plots instead of using DNA histograms. The reason for this lies in the cell count (density)–dependent display of the whole population as a third dimension in the plot. Depiction of relative frequencies correlated to the analyzed parameters facilitates proper discrimination between subsets. As an initial quality control step, however, we recommend performing back-gating or re-merging of gated subsets into DNA histograms in order to judge the overall accuracy of this initial gating step (**Supplementary Fig. 2b**). Moreover, G1, S and G2/M subsets can be discriminated via their specific FSC and SSC

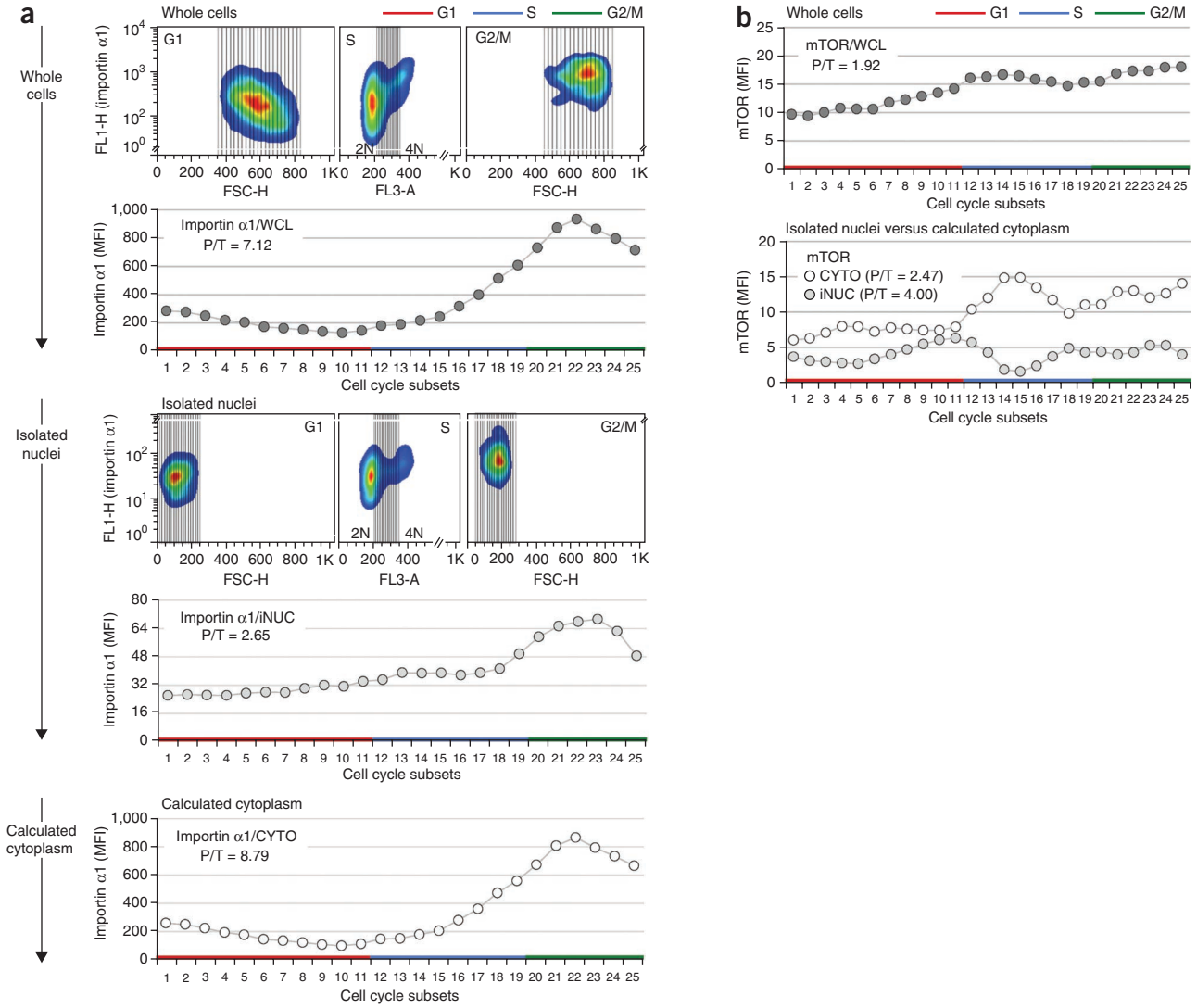

Figure 7 | Nucleocytoplasmic protein tracking throughout the cell cycle via improved flow cytometry. (**a**) Flow cytometric analyses of importin α1 cell cycle regulation in whole cells (WCL; top) and isolated nuclei (iNUC; middle), supplemented with thereof calculated data on the corresponding cytoplasmic regulation (bottom). For analyses of whole cells and isolated nuclei, Steps 2 and 3 of the gating procedure are presented (**Fig. 5a**). (**b**) Flow cytometry on the total (top) and nucleocytoplasmic (bottom) distribution of mTOR during the ongoing cell cycle. P/T ratios are indicated. CYTO, calculated cytoplasm.

properties, with G1 cells being smaller and less complex than G2/M cells. These differences can be easily visualized by re-merging subsets in a FSC/SSC dot plot and by directly comparing it with the whole population. Alternatively, FSC or SSC histograms of subsets can be re-merged and examined for the expected shifts (**Supplementary Figs. 2c** and **3a**).

? TROUBLESHOOTING

61| Display 2D pseudocolor plots of cell size (FSC-H) versus protein (FL1-H) for the G1 and G2/M subsets.

62| Further dissect cell cycle subsets using the rectangular gating tool. The area of drawn rectangles (termed FSC subsets) should be kept as small as possible to enable high resolution of the G1 and G2/M fractions and can be adjusted to the overall amount of analyzed cells. The more cells being analyzed, the more gates can be drawn. A minimum number of 80–100 cells per FSC subset was proven to yield reliable results (**Supplementary Fig. 3c**,**d**). Depending on the overall amount and the cell cycle distribution of analyzed cells, the absolute cell count per subset typically lies between 100 and 500 cells (G1) and 80 and 200 cells (G2/M), respectively (**Figs. 5a** and **7a**).

▲ **CRITICAL STEP** As there is no option to copy the rectangular gate within one plot, multiple gates must be drawn. Care should be taken to stick to the same gate size during this procedure to ensure homogenous distribution of cells in gates or subsets. Depending on the specific size distribution of the analyzed cell type, a minimum of 15–30 subsets per cell cycle

phase can be drawn. A screenshot of an FSC-dissected G1 subset is shown in **Supplementary Figure 3b**. The whole FSC gating procedure can be monitored for quality by displaying the specific FSC subset against its median FSC value. This is expected to yield almost linear, outlier-devoid curves, reflecting (to some extent) the continuous increase in cell size from G1 to G2/M. Alternatively, FSC subsets may be plotted against their corresponding SSC values. As SSC intensities were also shown to increase during cell cycle progression, this approach can be used to define outliers (most frequently caused by an insufficient number of cells (≤20) per subset being analyzed; **Supplementary Fig. 3c**,**d**).

63| Display the plot from Step 60 and delete the gates for G1 and G2/M while keeping the one for the S subset. Save this as a new file; otherwise, your initial G1/G2 gates will be lost for the whole workspace file.

64| Further dissect the S subset using the rectangular gating tool as described above. The area of drawn rectangles (now termed DNA subsets) should be kept as small as possible to enable high resolution. Typically, 9–15 gates are drawn. Depending on the overall amount and the cell cycle distribution of analyzed cells, the absolute cell count per subset lies between 200 and 800 cells (**Figs. 5a** and **7a**). At this point, it is notable that, although the S phase can also be efficiently FSC-dissected (**Supplementary Fig. 3**), information on S phase–specific protein expression is achieved by directly dissecting its DNA distribution. As the DNA amount of the S phase (in contrast to that of G1 and G2/M phases) directly reflects time-dependent changes in cell cycle progression (ranging from a ≥2N content of early S phase cells to a ≤4N content of late S phase cells), this is the straightest approach one can choose. An example illustrating a complete $FSC_{(G1)}/DNA_{(S)}/FSC_{(G2/M)}$ dissection is shown in **Supplementary Figure 4**.

65| Create a 2D pseudocolor plot of DNA (FL2 or 3-A) versus protein (FL1-H) and display the corresponding isotype control of the whole-cell population.

66| Copy the gates for G1, S and G2/M discrimination (Step 60) and paste them to the plot of the control sample. Only minor adjustments may be necessary.

67| Copy the gates for G1, S and G2/M dissection (Steps 62 and 64) and paste them to the corresponding plots of the control sample. Only minor adjustments may be necessary.

68| Perform Steps 59–67 for data on isolated nuclei, including the isotype controls. Gates for crude G1, S and G2/M discrimination (Step 60), as well as the gates for S phase dissection (Step 64), can be directly copied from the plots of whole-cell analyses and pasted to the plots of nuclei. Gates for G1 and G2/M dissection must be newly drawn (**Fig. 7a**).
▲ **CRITICAL STEP** As isolated nuclei have a more narrow size distribution than whole cells, the gate size has to be adjusted to approximately reach the actual number of gates (FSC subsets) set for the whole-cell population. Thus, a similar number of cells per FSC subset as well as a similar number of FSC subsets are analyzed in whole cells and isolated nuclei, which ensures similar cell size-dependent resolution of cell cycle phases between the populations being compared.

69| Retrieve the median fluorescence intensity ($FL1\text{-}H_{median}$ or median fluorescence intensity (MFI)) for each single subset of the $FSC_{(G1)}/DNA_{(S)}/FSC_{(G2/M)}$ dissection procedure by clicking the 'Add statistic' button. Apply this to dissected whole cells and isolated nuclei, stained with the specific antibody or the corresponding isotype controls.
▲ **CRITICAL STEP** In accordance with other flow cytometric studies, medians are used for quantification of results, as they are less prone to outliers than means[13,14]. In our experience, intra-assay variability is very low, and it is absolutely not necessary to perform duplicates or triplicates of reactions within a single experiment (e.g., triplicate staining of the same sample). Under these conditions, even consistency and reproducibility between independent experiments is high (e.g., data from two independent experiments on the phosphorylation of ribosomal protein S6 under conditions of dose-dependent mTOR inhibition in **Supplementary Fig. 5a**,**b**). However, as cell cycle– and localization-dependent protein expression and phosphorylation are generally very sensitive to slightly varying growth conditions (**Fig. 5b**)[16], we recommend first assaying under different growth conditions (e.g., varying time points of cell harvest after seeding) and performing two or three independent experiments under exactly the same conditions in order to obtain meaningful results.

70| Import data into Excel and correlate each FSC/DNA subset to its specific MFI. Include the total number of counts per subset.

71| Perform background correction by subtracting the MFIs of the isotype-stained sample from the corresponding MFIs of the specifically stained sample. Perform this step for all subsets of the whole cell and nuclei populations:

$$\mathrm{MFI}_{subset\ 1-X} = \mathrm{MFI}\_specific_{subset\ 1-X} - \mathrm{MFI}\_isotype_{subset\ 1-X}$$

This yields absolute fluorescence intensities, which are corrected for background staining and thus more truly reflect fold changes within the later calculated curves of cell cycle progression, and it considers and includes the fact that cell cycle subsets show slight differences in background staining. Both concerns are of particular importance when analyzing low signal intensities (e.g., weakly positive stainings).

72| Plot each cell cycle subset (the total of all FSC/DNA/FSC subsets) against its specific background-corrected MFI to obtain a single graph of the cell cycle–dependent expression of the specific protein of interest in whole cells and isolated nuclei, respectively.

73| Evaluate the overall quality of graphs and eliminate outliers. Outliers are easy to identify and are mostly due to the fact that the number of cells or nuclei per subset is too small to statistically give reliable results. For example, this is the case when the outermost regions of the dissected G1 and G2/M populations are analyzed. Depending on the overall amount of cells, we have observed these subsets to sometimes contain as few as ten cells, thereby causing a typical zig-zag graph pattern. Generally, the more the cells are analyzed, the lower the risk of perturbing outliers.
▲ CRITICAL STEP When outliers are eliminated, care has to be taken not to distort the balance in the number and distribution of cell cycle subsets between whole cells and isolated nuclei. As these reflect time-dependent changes during cell cycle progression, subsets identified and eliminated as outliers in the whole-cell graph have to be eliminated in the graph of isolated nuclei as well and vice versa. As another quality control step, we recommend determining the median of the total of all single MFIs of the dissected sample and comparing it with the MFI of the corresponding undissected sample. Deviations of less than 5% on average are typically observed. Deviations of more than 10% indicate balanced or unbalanced loss during the initial gating, subsequent dissection and/or final analysis steps. The overall quality of the procedure can also be evaluated by directly comparing the dissection results obtained for a exclusively nuclear marker protein such as topoisomerase IIβ: cell cycle graphs of whole cells and isolated nuclei are expected to yield very similar to almost identical patterns.
? TROUBLESHOOTING

74| Subtract the isotype-corrected MFIs of the outlier-adjusted and revised data set of isolated nuclei (iNUC) from the similarly processed set of whole cells (WCL) to yield results for the corresponding cytoplasmic expression (CYTO; **Fig. 7a**).

$$\mathrm{MFI}_{subset\ 1-X}[\mathrm{CYTO}] = \mathrm{MFI}_{subset\ 1-X}[\mathrm{WCL}] - \mathrm{MFI}_{subset\ 1-X}[\mathrm{iNUC}]$$

? TROUBLESHOOTING

75| Plot each cell cycle subset (the total of all FSC/DNA/FSC subsets) against its specific calculated MFI to obtain a single graph of the cell cycle–dependent expression of the specific protein of interest in the cytoplasm.

76| Display curves of cytoplasmic and nuclear regulations in one single graph to enable direct comparison to, e.g., identify cell cycle-dependent protein translocations. If fractions strongly differ in the absolute expression of a particular protein (e.g., high expression in the whole cell, low expression in the nucleus), simultaneous depiction of graphs may not be useful, as small fluctuations in the less-expressing population could be overlooked. Data sets may thus be normalized, with a particular subset (e.g., the initial subset as the earliest point in G1) being set to 1.0 and the other subsets being displayed in relation to it. This fold-change depiction enables direct comparison of data, although it is presented in two separate graphs.

77| Calculate the P/T (peak-to-trough) ratio for all fractions (WCL, iNUC and CYTO) to evaluate the overall extent of fluctuation during the cell cycle by dividing the highest MFI by the lowest:

$$\mathrm{P/T} = \mathrm{MFI}_{subset\ MAX} / \mathrm{MFI}_{subset\ MIN}$$

The higher the ratio, the higher the extent of fluctuation during cell cycle progression.

? TROUBLESHOOTING

Troubleshooting advice can be found in **Table 2**.

TABLE 2 | Troubleshooting table.

Step	Problem	Possible reason	Solution
5	Irreversible cell clumping	Excess trypsinization	Reduce the amount of trypsin-EDTA solution
			Shorten trypsin-EDTA incubation
			Increase the amount of serum-containing growth medium during the trypsin inactivation step
22	Excess, gradual loss of nuclear pellet during purification steps	Excessive nuclear breakage (cell type-dependent)	Adjust the amount of Nonidet P-40 substitute (0.1–1.0%, vol/vol)
			Avoid prolonged incubation in Nonidet P-40 substitute-supplemented extraction buffer A during washing steps
			Omit Nonidet P-40 substitute during washing steps
24B(ii)	Low nuclear yield	Inefficient homogenization	Avoid introduction of air bubbles
		Loss during purification	Reduce the number of washing steps
25	Aggregation of nuclei during fixation or permeabilization	Concentration of nuclei is too high	Predilute isolated nuclei in 1× PBS to a final concentration of 0.5×10^6 per ml (Step 26)
27	Loss of fixed nuclei	Inefficient pelleting	Use a centrifugal force ≥500*g*
44	Loss of nuclei during staining	Inappropriate handling	Use clear, low-retention tubes
			Mix by inverting, not by pipetting
58	Cytosolic contamination of nuclei	Inefficient cell lysis	Increase the amount of extraction buffer A
			Prolong hypotonic swelling
		Inefficient homogenization	Increase number of tip or needle strokes
		Inefficient purification	Increase amount of Nonidet P-40 substitute-supplemented extraction buffer A during washing steps
	Reduced nuclear integrity/nuclear leakage	Prolonged exposure to Nonidet P-40 substitute	Avoid prolonged incubation in Nonidet P-40 substitute-supplemented extraction buffer A during washing steps
			Omit Nonidet P-40 substitute during washing steps
60	Low quality of DNA staining (cytoplasmic staining; broadening of G1 and G2/M peaks)	Inappropriate fixation	Use electron microscopy–grade paraformaldehyde at final concentrations ≤1.5% (wt/vol)
		Inappropriate staining	Be sure to include an RNase digestion step when staining with propidium iodide
73	Excess amount of outliers	Too few cells per FSC/DNA subset	Eliminate subsets containing ≤80–100 cells or nuclei; acquire a minimum amount of 10,000 logarithmically growing cells for analysis
74	The antibody staining of isolated nuclei gives stronger signals than the corresponding whole cell staining (observed for exclusively or predominantely nuclear proteins)	Antibody dependent	Verify results using different antibodies targeting the same protein Co-analyze the nucleocytoplasmic distribution via immunoblotting using the fractions obtained with this protocol (Steps 18 and 23)

● TIMING

Steps 1–12, detachment and preparation of adherent cells for fractionation: ~15 min
Steps 13–24, isolation of pure, intact nuclei via biochemical fractionation: ~25–30 min
Steps 25–31, fixation and permeabilization of whole cells and isolated nuclei: ~20 min
Steps 32–45, protein and DNA staining of whole cells and isolated nuclei: ~2.5 h
Steps 46–53, data acquisition on the flow cytometer: ~1 h
Steps 54–77, data analysis and calculation: ~3–5 h

ANTICIPATED RESULTS

Purity and integrity of isolated nuclei

As an initial quality control step, freshly isolated nuclei are examined under the microscope. Pure, intact nuclei are largely free from the surrounding cytoplasm, are similar in size when compared with *in situ* nuclei, have a slightly shiny contour and do not show excessive aggregation (**Fig. 1a**,**b**). When analyzed for the specific size distribution via the CASY cell counter and analyzer (or similar equipment), the nuclear fraction shows up as a nearly 100% enriched fraction of particles of substantially smaller size. Excessive aggregation of isolated nuclei, detected by skewing of the otherwise symmetric distribution toward the right (increased particle size due to multiple nuclei sticking together), is usually not observed (**Fig. 1c**). **Figure 2a**,**b** shows the anticipated results in terms of nuclear purity, if optional immunoblotting analyses of nuclear and co-extracted cytoplasmic fractions are performed.

Nuclei that are further processed for flow cytometry (**Figs. 1a** and **3**) are thoroughly examined for purity and integrity, using a defined panel of subcellular marker proteins. **Figure 4a** illustrates the different subcellular layers and corresponding marker proteins covered by this specific panel. High-quality fractionation yields nuclei that are entirely free from cytoplasmic contamination, evaluated via analyses of cytoskeletal, cytosolic and nuclear membrane–associated proteins including tubulins, HSP90 and calnexin (**Fig. 4b**). Whole cells and nuclei show comparable results when analyzed for nuclear marker proteins, including nucleolar (fibrillarin), nucleoplasmic (CENP-A, topoisomerase IIβ), nuclear lamina (lamin A/C) and nuclear pore proteins (NUP98), with the latter representing the outermost nuclear layer and thus being a particularly sensitive parameter. Increased loss of nuclear material as a result of nuclear leakiness, evidenced by a major decrease in nuclear compared with whole-cell signal intensities, is not observed (**Fig. 4b**). This highly stringent approach of assessing multiple subcellular layers is necessary in order to verify the quality of the nuclear preparation. Finally, G1 and G2/M subsets of whole cells and isolated nuclei have anticipated differences in size (**Fig. 4c**). Taken together, these results confirm the overall applicability of isolated nuclei for the intended flow cytometric approach.

Data analysis, verification and interpretation

The overall utility of our approach to identifying cell cycle–regulated events, with respect to both specificity and sensitivity, was verified by analyzing known cell cyle–regulated proteins in different cells, including hAFS cells, immortalized MEFs and BxPC-3 human pancreas carcinoma cells (see also **Supplementary Figs. 8–12**). By using a classic synchronization approach followed by immunoblotting and densitometric analyses, CENP-A (histone H3-like centromeric protein A) expression was observed to peak in G2/M phase[37]. **Figure 5a** includes the main steps of the gating procedure and the results of data alignment in the investigation of CENP-A cell cycle regulation in Q1 hAFS cells using our modified approach. As demonstrated, our assay was fully capable of recapitulating the characteristic pattern of G2/M peak expression. We performed similar confirmation experiments for the expression of histone H3 and α-tubulin (**Supplementary Fig. 8**). To test the sensitivity of our method, we continued with an approach that was more susceptible to different or varying growth conditions: the CDK inhibitor p27 is well known to have both cell cycle regulatory properties and cell cycle–dependent expression. It has been shown that its increased expression under reduced growth conditions depends on tuberin (*TSC2*)[38,39]. By analyzing p27 expression in $TSC2^{+/+}$ and $TSC2^{-/-}$ MEFs cultured under three different growth conditions, we were able to also detect the more subtle, TSC2- and growth-dependent differences in p27 expression during unperturbed cell cycle progression (**Fig. 5b** and **Supplementary Fig. 9**). Collectively, data presented in this figure show the feasibility of our approach to detecting cell cycle–regulated events of varying extents. **Figure 6** outlines the basic principle of data evaluation when whole cells and isolated nuclei are coanalyzed. Exclusive cytoplasmic (HSP90) or nuclear (lamin A/C) localization can be easily identified, with intermediate states being representative of nucleocytoplasmic distribution (importin α1, mTOR; **Fig. 6a**; see also **Fig. 4b** and **Supplementary Fig. 10**). Upon subtraction of nuclear from whole cell results, information on the corresponding cytoplasmic expression is obtained (**Fig. 6b**). As an option, results can be verified by coanalyzing cytoplasmic and nuclear fractions via immunoblotting. **Figure 6c** shows the immunoblot outcome for the nucleocytoplasmic distribution of HSP90, importin α1 and mTOR, cytofluorometrically analyzed in **Figure 6a**,**b**.

This approach is finally applied to the analysis of protein expression during cell cycle progression. We show (**Fig. 7a** and **Supplementary Fig. 11a**) a complete cycle of analyses to evaluate the distribution of the nucleocytoplasmic shuttling protein importin α1, which is known to show cell cycle–dependent regulation but for which information on the corresponding nucleocytoplasmic expression has thus far been unavailable[40]. On comparing patterns of mTOR expression obtained via serum

starvation/re-stimulation (**Fig. 2d**)[11] and our refined protocol (**Fig. 7b**), the following conclusion can be drawn: strongly induced expression of nuclear mTOR during G1 progression and its rapid decline at the G1/S transition is detected by both methods. This holds true for the slight induction of cytoplasmic mTOR during early G1, indicating that these patterns reflect true, cell cycle–dependent regulations rather than being a consequence of the serum response during re-stimulation. However, as synchrony rapidly declines at the G1/S transition, information on the expression in S and G2/M phases of the cell cycle is limited (**Fig. 2d**) but can ultimately be obtained using this refined flow cytometry approach (**Fig. 7b** and **Supplementary Fig. 11b**).

Note: Supplementary information is available in the online version of the paper.

ACKNOWLEDGMENTS The clonal human amniotic fluid stem cell line Q1 was kindly provided by A. Atala (Wake Forest University School of Medicine). *CDKN1B* (p27), *TSC2* (tuberin) and *TOP2B* (topoisomerase IIβ) wild-type and knockout cells were obtained from J.M. Roberts (Fred Hutchinson Cancer Research Center), D.J. Kwiatkowski (Brigham and Women's Hospital) and N. Adachi (Yokohama City University), respectively. We thank all members of our laboratory for helpful comments and discussion.

AUTHOR CONTRIBUTIONS M.R. and K.S. designed and performed experiments, analyzed data and wrote the article. M.H. conceived the method, designed experiments, analyzed data and wrote the article.

COMPETING FINANCIAL INTERESTS The authors declare no competing financial interests.

Published online at http://www.nature.com/doifinder/10.1038/nprot.2013.011. Reprints and permissions information is available online at http://www.nature.com/reprints/index.html.

1. Scott, J.D. & Pawson, T. Cell signaling in space and time: where proteins come together and when they're apart. *Science* **326**, 1220–1224 (2009).
2. Murphy, L.O. & Blenis, J. MAPK signal specificity: the right place at the right time. *Trends Biochem. Sci.* **31**, 268–275 (2006).
3. Zaidi, S.K. *et al.* Nuclear microenvironments in biological control and cancer. *Nat. Rev. Cancer* **7**, 454–463 (2007).
4. Rajendran, L., Knölker, H.J. & Simons, K. Subcellular targeting strategies for drug design and delivery. *Nat. Rev. Drug Discov.* **9**, 29–42 (2010).
5. Rosner, M., Schipany, K. & Hengstschläger, M. Spatial consequences of blocking mTOR/S6K: relevance for therapy. *Cell Cycle* **11**, 420–421 (2012).
6. Keyomarsi, K. & Pardee, A.B. Selective protection of normal proliferating cells against the toxic effects of chemotherapeutic agents. *Prog. Cell Cycle Res.* **5**, 527–532 (2003).
7. Laplante, M. & Sabatini, D.M. mTOR signaling in growth control and disease. *Cell* **149**, 274–292 (2012).
8. Rosner, M. & Hengstschläger, M. Cytoplasmic and nuclear distribution of the protein complexes mTORC1 and mTORC2: rapamycin triggers dephosphorylation and delocalization of the mTORC2 components rictor and sin1. *Hum. Mol. Genet.* **17**, 2934–2948 (2008).
9. Roblek, M. *et al.* Monoclonal antibodies specific for disease-associated point-mutants: lamin A/C R453W and R482W. *PLoS ONE* **5**, e10604 (2010).
10. Rosner, M. & Hengstschläger, M. Nucleocytoplasmic localization of p70 S6K1, but not of its isoforms p85 and p31, is regulated by TSC2/mTOR. *Oncogene* **30**, 4509–4522 (2011).
11. Rosner, M. & Hengstschläger, M. mTOR protein localization is cell cycle-regulated. *Cell Cycle* **15**, 3608–3610 (2011).
12. Roederer, M. Multiparameter FACS analysis. *Curr. Protoc. Immunol.* **49**, 5.8.1–5.8.10 (2002).
13. Krutzik, P.O., Crane, J.M., Clutter, M.R. & Nolan, G.P. High-content single-cell drug screening with phosphospecific flow cytometry. *Nat. Chem. Biol.* **4**, 132–142 (2007).
14. Krutzik, P.O., Trejo, A., Schulz, K.R. & Nolan, G.P. Phospho flow cytometry methods for the analysis of kinase signaling in cell lines and primary human blood samples. *Methods Mol. Biol.* **699**, 179–202 (2011).
15. Darzynkiewicz, Z., Juan, G. & Traganos, F. Cytometry of cell cycle regulatory proteins. *Prog. Cell Cycle Res.* **5**, 533–542 (2003).
16. Rosner, M., Schipany, K. & Hengstschläger, M. Phosphorylation of nuclear and cytoplasmic pools of ribosomal protein S6 during cell cycle progression. *Amino Acids* doi:10.1007/s00726-012-1445-1 (20 December 2012).
17. Conlon, I.J., Dunn, G.A., Mudge, A.W. & Raff, M.C. Extracellular control of cell size. *Nat. Cell Biol.* **3**, 918–921 (2003).
18. Mitchison, J.M. Growth during the cell cycle. *Int. Rev. Cytol.* **226**, 165–258 (2003).
19. Huber, M.D. & Gerace, L. The size-wise nucleus: nuclear volume control in eukaryotes. *J. Cell Biol.* **179**, 583–584 (2007).
20. Maeshima, K., Iino, H., Hihara, S. & Imamoto, N. Nuclear size, nuclear pore number and cell cycle. *Nucleus* **2**, 113–118 (2011).
21. Pardee, A.B. & Keyomarsi, K. Modification of cell proliferation with inhibitors. *Curr. Opin. Cell Biol.* **4**, 186–191 (1992).
22. Davis, P.K., Ho, A. & Dowdy, S.F. Biological methods for cell-cycle synchronization of mammalian cells. *Biotechniques* **30**, 1322–1326 (2001).
23. Jackmann, J. & O'Connor, P.M. Methods for synchronizing cells at specific stages of the cell cycle. *Curr. Protoc. Cell Biol.* **8.3**, 8.3.1–8.3.20 (2001).
24. Harper, J.V. Synchronization of cell populations in G1/S and G2/M phases of the cell cycle. *Methods Mol. Biol.* **296**, 157–166 (2005).
25. Banfalvi, G. Overview of cell synchronization. *Methods Mol. Biol.* **761**, 1–23 (2011).
26. Kung, A.L., Zetterberg, A., Sherwood, S.W. & Schimke, R.T. Cytotoxic effects of cell cycle phase specific agents: result of cell cycle perturbation. *Cancer Res.* **50**, 7307–7317 (1990).
27. Urbani, L., Sherwood, S.W. & Schimke, R.T. Dissociation of nuclear and cytoplasmic cell cycle progression by drugs employed in cell synchronization. *Exp. Cell Res.* **219**, 159–168 (1995).
28. Gong, J., Traganos, F. & Darzynkiewicz, Z. Growth imbalance and altered expression of cyclins B1, A, E, and D3 in MOLT-4 cells synchronized in the cell cycle by inhibitors of DNA replication. *Cell Growth Differ.* **6**, 1485–1493 (1995).
29. Darzynkiewicz, Z., Halicka, H.D., Zhao, H. & Podhorecka, M. Cell synchronization by inhibitors of DNA replication induces replication stress and DNA damage response: analysis by flow cytometry. *Methods Mol. Biol.* **761**, 85–96 (2011).
30. Miloloza, A. *et al.* The *TSC1* gene product, hamartin, negatively regulates cell proliferation. *Hum. Mol. Genet.* **9**, 1721–1727 (2000).
31. Soucek, T., Pusch, O., Wienecke, R., DeClue, J.E. & Hengstschläger, M. Role of the tuberous sclerosis gene-2 product in cell cycle control. Loss of the tuberous sclerosis gene-2 induces quiescent cells to enter S phase. *J. Biol. Chem.* **272**, 29301–29308 (1997).
32. Astrinidis, A., Senapedis, W., Coleman, T.R. & Henske, E.P. Cell cycle-regulated phosphorylation of hamartin, the product of the tuberous sclerosis complex 1 gene, by cyclin-dependent kinase 1/cyclin B. *J. Biol. Chem.* **278**, 51372–51379 (2003).
33. De Coppi, P. *et al.* Isolation of amniotic stem cell lines with potential for therapy. *Nat. Biotechnol.* **25**, 100–106 (2007).
34. Rosner, M. *et al.* Efficient siRNA-mediated prolonged gene silencing in human amniotic fluid stem cells. *Nat. Protoc.* **5**, 1081–1095 (2010).
35. Rosner, M. & Hengstschläger, M. Cytoplasmic/nuclear localization of tuberin in different cell lines. *Amino Acids* **33**, 575–579 (2007).
36. Rosner, M., Freilinger, A. & Hengstschläger, M. Akt regulates nuclear/cytoplasmic localization of tuberin. *Oncogene* **26**, 521–531 (2007).
37. Shelby, R.D., Monier, K. & Sullivan, K.F. Chromatin assembly at kinetochores is uncoupled from DNA replication. *J. Cell Biol.* **151**, 1113–1118 (2000).
38. Soucek, T., Yeung, R. & Hengstschläger, M. Inactivation of the cyclin-dependent kinase inhibitor p27 upon loss of the tuberous sclerosis complex gene-2. *Proc. Natl. Acad. Sci. USA* **95**, 15653–15658 (1998).
39. Rosner, M. & Hengstschläger, M. Tuberin binds p27 and negatively regulates its interaction with the SCF component Skp2. *J. Biol. Chem.* **279**, 48707–48715 (2004).
40. Zhu, W., Giangrande, P.H. & Nevins, J.R. E2Fs link the control of G1/S and G2/M transcription. *EMBO J.* **23**, 4615–4626 (2004).
41. Keyomarsi, K., Sandoval, L., Band, V. & Pardee, A.B. Synchronization of tumor and normal cells from G1 to multiple cell cycles by lovastatin. *Cancer Res.* **51**, 3602–3609 (1991).
42. Hengst, L., Dulic, V., Slingerland, J.M., Lees, E. & Reed, S.I. A cell cycle-regulated inhibitor of cyclin-dependent kinases. *Proc. Natl. Acad. Sci. USA* **91**, 5291–5295 (1994).
43. Rao, S. *et al.* Lovastatin-mediated G1 arrest is through inhibition of the proteasome, independent of hydroxymethyl glutaryl-CoA reductase. *Proc. Natl. Acad. Sci. USA* **96**, 7797–7802 (1999).

44. Javanmoghadam-Kamrani, S. & Keyomarsi, K. Synchronization of the cell cycle using lovastatin. *Cell Cycle* **7**, 2434–2440 (2008).
45. Lalande, M. A reversible arrest point in the late G1 phase of the mammalian cell cycle. *Exp. Cell Res.* **186**, 332–339 (1990).
46. Kalejta, R.F. & Hamlin, J.L. The dual effect of mimosine on DNA replication. *Exp. Cell Res.* **231**, 173–183 (1997).
47. Marraccino, R.L., Firpo, E.J. & Roberts, J.M. Activation of the p34 CDC2 protein kinase at the start of S phase in the human cell cycle. *Mol. Biol. Cell* **3**, 389–401 (1992).
48. Park, S.Y. *et al.* Mimosine arrests the cell cycle prior to the onset of DNA replication by preventing the binding of human Ctf4/And-1 to chromatin via Hif-1α activation in HeLa cells. *Cell Cycle* **11**, 761–766 (2012).
49. Bootsma, D., Budke, L. & Vos, O. Studies on synchronous division of tissue culture cells initiated by excess thymidine. *Exp. Cell Res.* **33**, 301–309 (1964).
50. Thomas, D.B. & Lingwood, C.A. A model of cell cycle control: effects of thymidine on synchronous cell cultures. *Cell* **5**, 37–42 (1975).
51. Mittnacht, S. & Weinberg, R.A. G1/S phosphorylation of the retinoblastoma protein is associated with an altered affinity for the nuclear compartment. *Cell* **65**, 381–393 (1991).
52. Whitfield, M.L. *et al.* Identification of genes periodically expressed in the human cell cycle and their expression in tumors. *Mol. Biol. Cell* **13**, 1977–2000 (2002).
53. Ikegami, S. *et al.* Aphidicolin prevents mitotic cell division by interfering with the activity of DNA polymerase-α. *Nature* **275**, 458–460 (1978).
54. Pedrali-Noy, G. *et al.* Synchronization of HeLa cell cultures by inhibition of DNA polymerase αwith aphidicolin. *Nucleic Acids Res.* **8**, 377–387 (1980).
55. Dulić V., Stein, G.H., Far, D.F. & Reed, S.I. Nuclear accumulation of p21Cip1 at the onset of mitosis: a role at the G2/M-phase transition. *Mol. Cell Biol.* **18**, 546–557 (1998).
56. Adams, R.L. & Lindsay, J.G. Hydroxyurea reversal of inhibition and use as a cell-synchronizing agent. *J. Biol. Chem.* **242**, 1314–1317 (1967).
57. Maurer-Schultze, B., Siebert, M. & Bassukas, I.D. An *in vivo* study on the synchronizing effect of hydroxyurea. *Exp. Cell Res.* **174**, 230–243 (1988).
58. Ishida, S. *et al.* Role for E2F in control of both DNA replication and mitotic functions as revealed from DNA microarray analysis. *Mol. Cell Biol.* **21**, 4684–4699 (2001).
59. Taylor, E.W. The mechanism of colchicine inhibition of mitosis. I. Kinetics of inhibition and the binding of h3-colchicine. *J. Cell Biol.* **25**, 145–160 (1965).
60. Romsdahl, M.M. Synchronization of human cell lines with colcemid. *Exp. Cell Res.* **50**, 463–467 (1968).
61. Sherwood, S.W., Rush, D.F., Kung, A.L. & Schimke, R.T. Cyclin B1 expression in HeLa S3 cells studied by flow cytometry. *Exp. Cell Res.* **211**, 275–281 (1994).
62. Hayashi, M.T., Cesare, A.J., Fitzpatrick, J.A., Lazzerini-Denchi, E. & Karlseder, J. A telomere-dependent DNA damage checkpoint induced by prolonged mitotic arrest. *Nat. Struct. Mol. Biol.* **19**, 387–394 (2012).
63. Deysson, G. Antimitotic substances. *Int. Rev. Cytol.* **24**, 99–148 (1968).
64. Zieve, G.W., Turnbull, D., Mullins, J.M. & McIntosh, J.R. Production of large numbers of mitotic mammalian cells by use of the reversible microtubule inhibitor nocodazole. Nocodazole accumulated mitotic cells. *Exp. Cell Res.* **126**, 397–405 (1980).
65. Jansen-Dürr, P. *et al.* Differential modulation of cyclin gene expression by MYC. *Proc. Natl. Acad. Sci. USA* **90**, 3685–3689 (1993).
66. Matsui, Y., Nakayama, Y., Okamoto, M., Fukumoto, Y. & Yamaguchi, N. Enrichment of cell populations in metaphase, anaphase, and telophase by synchronization using nocodazole and blebbistatin: a novel method suitable for examining dynamic changes in proteins during mitotic progression. *Eur. J. Cell Biol.* **91**, 413–419 (2012).
67. Griffin, M.J. Synchronization of some human cell strains by serum and calcium starvation. *In Vitro* **12**, 393–398 (1976).
68. Campisi, J., Morreo, G. & Pardee, A.B. Kinetics of G1 transit following brief starvation for serum factors. *Exp. Cell Res.* **152**, 459–466 (1984).
69. Pardee, A.B. G1 events and regulation of cell proliferation. *Science* **246**, 603–608 (1989).
70. Pagano, M. *et al.* Role of the ubiquitin-proteasome pathway in regulating abundance of the cyclin-dependent kinase inhibitor p27. *Science* **269**, 682–685 (1995).
71. Langan, T.J. & Chou, R.C. Synchronization of mammalian cell cultures by serum deprivation. *Methods Mol. Biol.* **761**, 75–83 (2011).
72. Tobey, R.A. & Crissman, H.A. Preparation of large quantities of synchronized mammalian cells in late G1 in the pre-DNA replicative phase of the cell cycle. *Exp. Cell Res.* **75**, 460–464 (1972).
73. Ley, K.D. & Murphy, M.M. Synchronization of mitochondrial DNA synthesis in Chinese hamster cells (line CHO) deprived of isoleucine. *J. Cell Biol.* **58**, 340–345 (1973).
74. Cifuentes, E., Croxen, R., Menon, M., Barrack, E.R. & Reddy, G.P. Synchronized prostate cancer cells for studying androgen-regulated events in cell cycle progression from G1 into S phase. *J. Cell Physiol.* **195**, 337–345 (2003).
75. Holley, R.W. & Kiernan, J.A. 'Contact inhibition' of cell division in 3T3 cells. *Proc. Natl. Acad. Sci. USA* **60**, 300–304 (1968).
76. Polyak, K. *et al.* p27Kip1, a cyclin-Cdk inhibitor, links transforming growth factor-β and contact inhibition to cell cycle arrest. *Genes Dev.* **8**, 9–22 (1994).
77. Nelson, P.J. & Daniel, T.O. Emerging targets: molecular mechanisms of cell contact-mediated growth control. *Kidney Int.* **61**, S99–S105 (2002).
78. Haberichter, T. *et al.* A systems biology dynamical model of mammalian G1 cell cycle progression. *Mol. Syst. Biol.* **3**, 84 (2007).
79. Elvin, P. & Evans, C.W. Cell adhesiveness and the cell cycle: correlation in synchronized BALB/c 3T3 cells. *Biol. Cell* **48**, 1–9 (1983).
80. Morla, A.O., Draetta, G., Beach, D. & Wang, J.Y. Reversible tyrosine phosphorylation of cdc2: dephosphorylation accompanies activation during entry into mitosis. *Cell* **58**, 193–203 (1989).
81. Schorl, C. & Sedivy, J.M. Analysis of cell cycle phases and progression in cultured mammalian cells. *Methods* **41**, 143–150 (2007).
82. Beyrouthy, M.J. *et al.* Identification of G1-regulated genes in normally cycling human cells. *PLoS ONE* **3**, e3943 (2008).
83. Lindahl, P.E. Principle of a counter-streaming centrifuge for the separation of particles of different sizes. *Nature* **161**, 648 (1948).
84. Kauffman, M.G., Noga, S.J., Kelly, T.J. & Donnenberg, A.D. Isolation of cell cycle fractions by counterflow centrifugal elutriation. *Anal. Biochem.* **191**, 41–46 (1990).
85. Dulić, V., Lees, E. & Reed, S.I. Association of human cyclin E with a periodic G1-S phase protein kinase. *Science* **257**, 1958–1961 (1992).
86. Zickert, P., Wejde, J., Skog, S., Zetterberg, A. & Larsson, O. Growth-regulatory properties of G1 cells synchronized by centrifugal elutriation. *Exp. Cell Res.* **207**, 115–121 (1993).
87. Hengstschläger, M., Pusch, O., Soucek, T., Hengstschläger-Ottnad, E. & Bernaschek, G. Quality control of centrifugal elutriation for studies of cell cycle regulations. *Biotechniques* **23**, 232–234, 236–237 (1997).
88. Banfalvi, G. Cell cycle synchronization of animal cells and nuclei by centrifugal elutriation. *Nat. Protoc.* **3**, 663–673 (2008).
89. Arndt-Jovin, D.J. & Jovin, T.M. Analysis and sorting of living cells according to deoxyribonucleic acid content. *J. Histochem. Cytochem.* **25**, 585–589 (1977).
90. Widrow, R.J. & Laird, C.D. Enrichment for submitotic cell populations using flow cytometry. *Cytometry* **39**, 126–130 (2000).
91. Juan, G., Hernando, E. & Cordon-Cardo, C. Separation of live cells in different phases of the cell cycle for gene expression analysis. *Cytometry* **49**, 170–175 (2002).
92. Coquelle, A. *et al.* Enrichment of non-synchronized cells in the G1, S and G2 phases of the cell cycle for the study of apoptosis. *Biochem. Pharmacol.* **72**, 1396–1404 (2006).
93. Shapiro, H.M. *Practical Flow Cytometry*. John Wiley & Sons, 2003.
94. Darzynkiewicz, Z. *et al.* Features of apoptotic cells measured by flow cytometry. *Cytometry* **13**, 795–808 (1992).
95. Freilinger, A. *et al.* Tuberin activates the proapoptotic molecule BAD. *Oncogene* **25**, 6467–6479 (2006).
96. Zhang, H., Stallock, J.P., Ng, J.C., Reinhard, C. & Neufeld, T.P. Regulation of cellular growth by the *Drosophila* target of rapamycin dTOR. *Genes Dev.* **14**, 2712–2724 (2000).
97. Fingar, D.C., Salama, S., Tsou, C., Harlow, E. & Blenis, J. Mammalian cell size is controlled by mTOR and its downstream targets S6K1 and 4EBP1/eIF4E. *Genes Dev.* **16**, 1472–1487 (2002).
98. Rosner, M., Hofer, K., Kubista, M. & Hengstschläger, M. Cell size regulation by the human TSC tumor suppressor proteins depends on PI3K and FKBP38. *Oncogene* **22**, 4786–4798 (2003).
99. Murakami, M. *et al.* mTOR is essential for growth and proliferation in early mouse embryos and embryonic stem cells. *Mol. Cell Biol.* **24**, 6710–6718 (2004).
100. Ruvinsky, I. *et al.* Ribosomal protein S6 phosphorylation is a determinant of cell size and glucose homeostasis. *Genes Dev.* **19**, 2199–1211 (2005).
101. Rosner, M., Fuchs, C., Siegel, N., Valli, A. & Hengstchläger, M. Functional interaction of mammalian target of rapamycin complexes in regulating mammalian cell size and cell cycle. *Hum. Mol. Genet.* **18**, 3298–3310 (2009).
102. Ekim, B. *et al.* mTOR kinase domain phosphorylation promotes mTORC1 signaling, cell growth, and cell cycle progression. *Mol. Cell Biol.* **31**, 2787–2801 (2011).

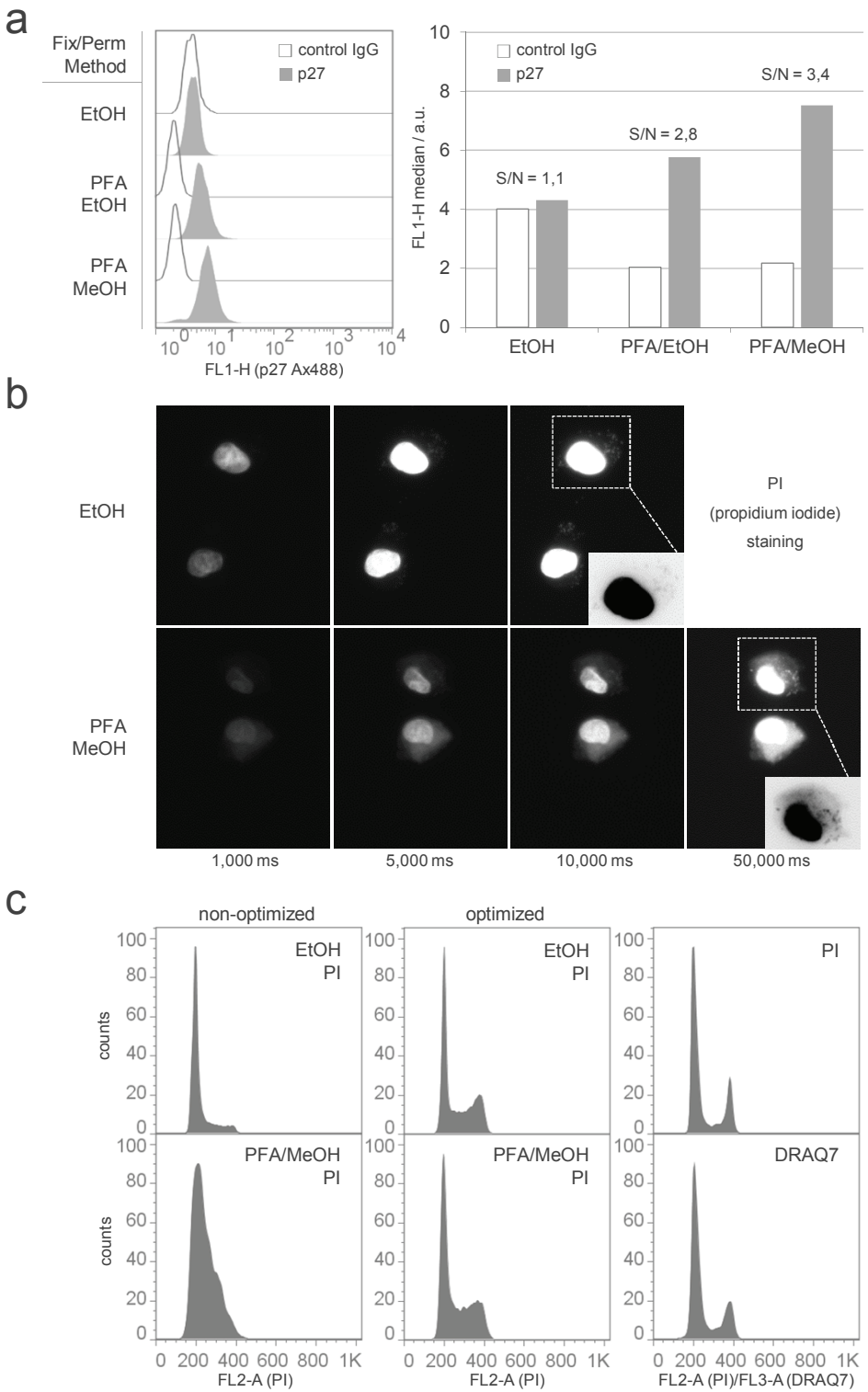

Optimized fixation conditions for the combined analysis of DNA and protein on the flow cytometer.

(a) *Left:* Q1 hAFS cells, fixed and permeabilized with either ethanol (*EtOH*), a combination of paraformaldehyde and ethanol (*PFA/EtOH*) or paraformaldehyde and methanol (*PFA/MeOH*), were stained for p27 and analysed on the flow cytometer. *Right:* Graph depiction of corresponding median fluorescence values. S/N (*Signal-to-Noise*) ratios are indicated. **(b)** Representativ pictures of EtOH and PFA/MeOH-fixed cells stained for DNA with propidium iodide (*ms*, exposure time in milliseconds). For better visualization, framed areas were magnified and inverted. **(c)** *Left* (*top and bottom*): Flow cytometric analyses of PI-stained cells shown in b. *Middle* (*top and bottom*): PI-staining and analysis using optimized fixation conditions (for details see the PROCEDURE). *Right* (*top and bottom*): comparative staining of DNA under optimized fixation conditions using either propidium iodide or DRAQ7.

Nature Protocols: doi: 10.1038/nprot.2013.011

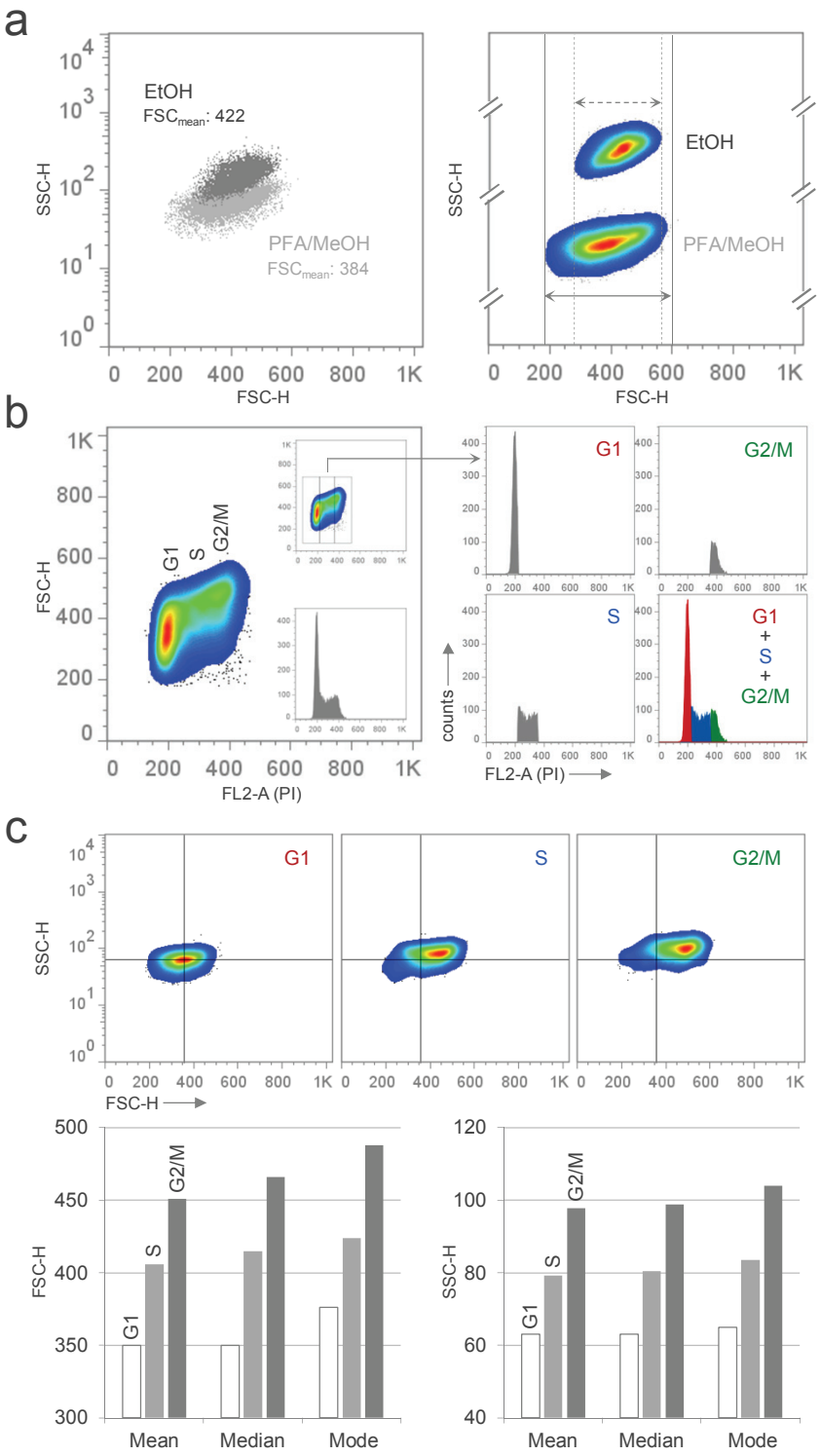

Evaluation of FSC (forward scatter) analyses to study cell cycle-associated changes in cell size. **(a)** *Left*: Overlay of FSC (forward scatter) versus SSC (side scatter) dot plots showing *TSC2*$^{+/+}$ mouse embryonic fibroblasts, either fixed with ethanol (*EtOH*) or paraformaldehyde/methanol (*PFA/MeOH*). Mean FSC values (*FSC$_{mean}$*) are indicated. *Right:* Smoothed versions of the same plots which were cropped and re-merged one below the other to allow better comparison of FSC distribution (double rules indicate sites of cropping). **(b)** 2-D (two-dimensional) gating for G1, S and G2/M cell cycle subsets. *Left:* Two-dimensional dot plot displaying FSC (cell size) versus FL2-A (DNA content) of PFA/MeOH-fixed and propidium iodide-stained cells. The imprint at the top shows the same plot including the gates to separate G1, S and G2/M subsets. The imprint at the bottom shows the corresponding DNA histogram. *Right:* Histogram depiction of single and re-merged cell cycle subsets. **(c)** Forward/Side scatter analyses of cell cycle subsets. *Top:* Two-dimensional dot plots showing FSC and SSC intensities of G1, S and G2/M subsets. A quad gate was set into the center of the G1 subset and copied to adjacent plots to better visualize FSC and SSC shifts in S and G2/M subsets. *Bottom:* Graph depiction of the corresponding mean, median and mode (peak) FSC (*left*) and SSC (*right*) values.

Nature Protocols: doi: 10.1038/nprot.2013.011

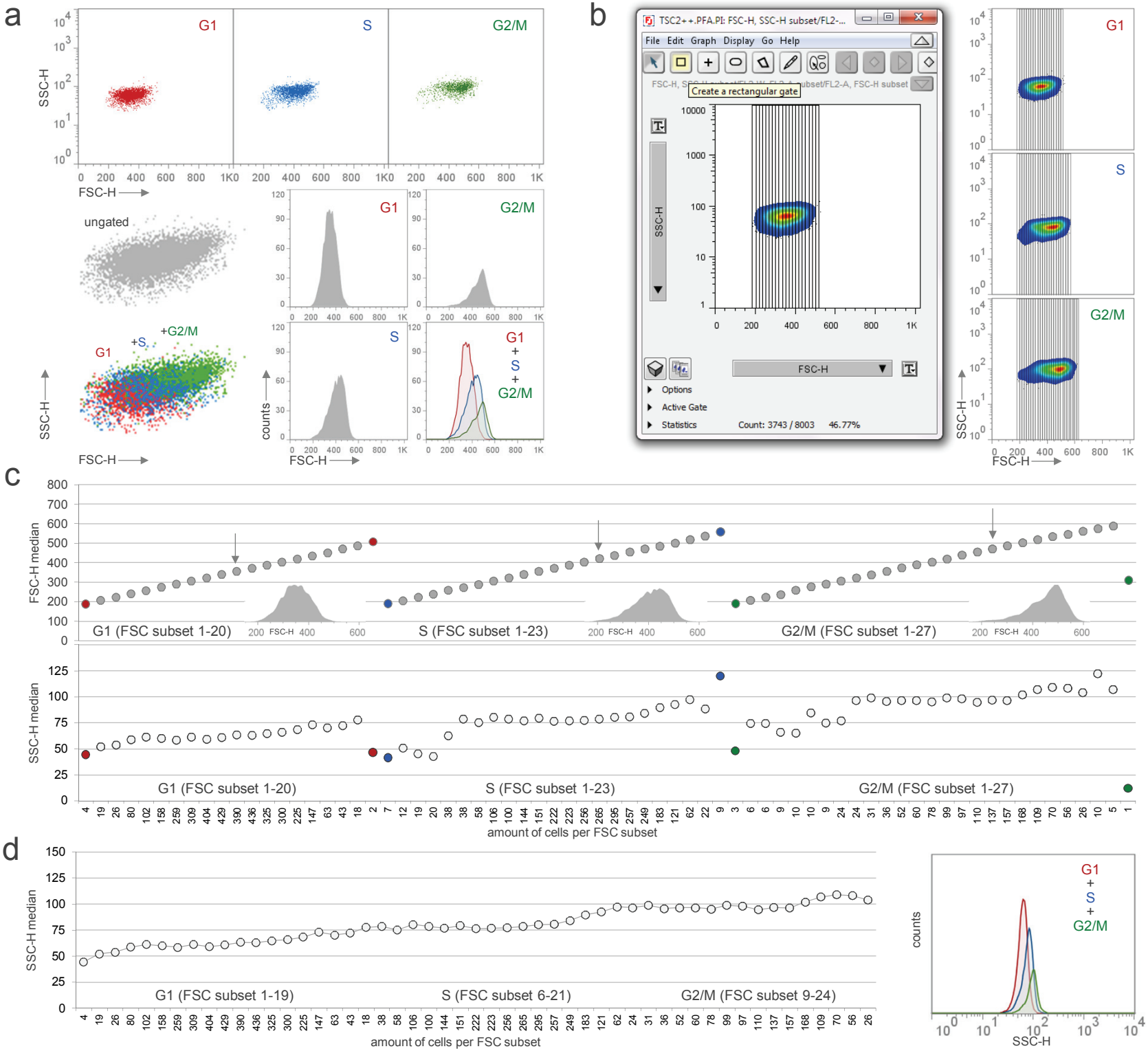

Approach and quality control of FSC (forward scatter) dissection.

(a) Preliminary quality control of the G1, S and G2/M gating process with respect to obtained FSC results. Under appropriate fixation conditions (as the ones described here) G1, S and G2/M subsets of MEFs display described differences in FSC and SSC properties (*top*) which can be readily visualized by re-merging subsets in a FSC/SSC dot plot and by directly comparing it with the (*ungated*) whole population (*bottom, left*). Alternatively, FSC histograms of subsets can be re-merged and examined for the expected shift (*bottom, right*). **(b)** Approach of FSC dissection. Using a software-based, rectangular gating tool, cell cycle subsets are further dissected according to their FSC (size) distribution. A screenshot of a so dissected G1 subset is presented (*left*). According to the specific size distribution of the different cell cycle phases (and depending on the cell type) varying amounts of FSC subsets can be drawn ranging from 20 to as much as 30 per subset yielding a very high resolution (*right*). **(c)** As part of the quality control each single FSC subset is displayed against its corresponding median FSC value what is expected to yield almost linear distributions for each cell cycle phase (*top*). Arrows indicate the median FSC of each cell cycle phase. Coloured dots label the very first and very last FSC subset of each cell cycle phase. As the SSC as well constantly increases from G1 to M, a correlation of obtained FSC subsets with corresponding SSC values can help to identify potential outliers (e.g. too little cells per subset giving unreliable results) (*bottom*). **(d)** *Left:* Outlier-adjusted, high resolution graph showing the cell cycle-associated increase in SSC. *Right:* SSC histogram of re-merged cell cycle subsets.

Nature Protocols: doi: 10.1038/nprot.2013.011

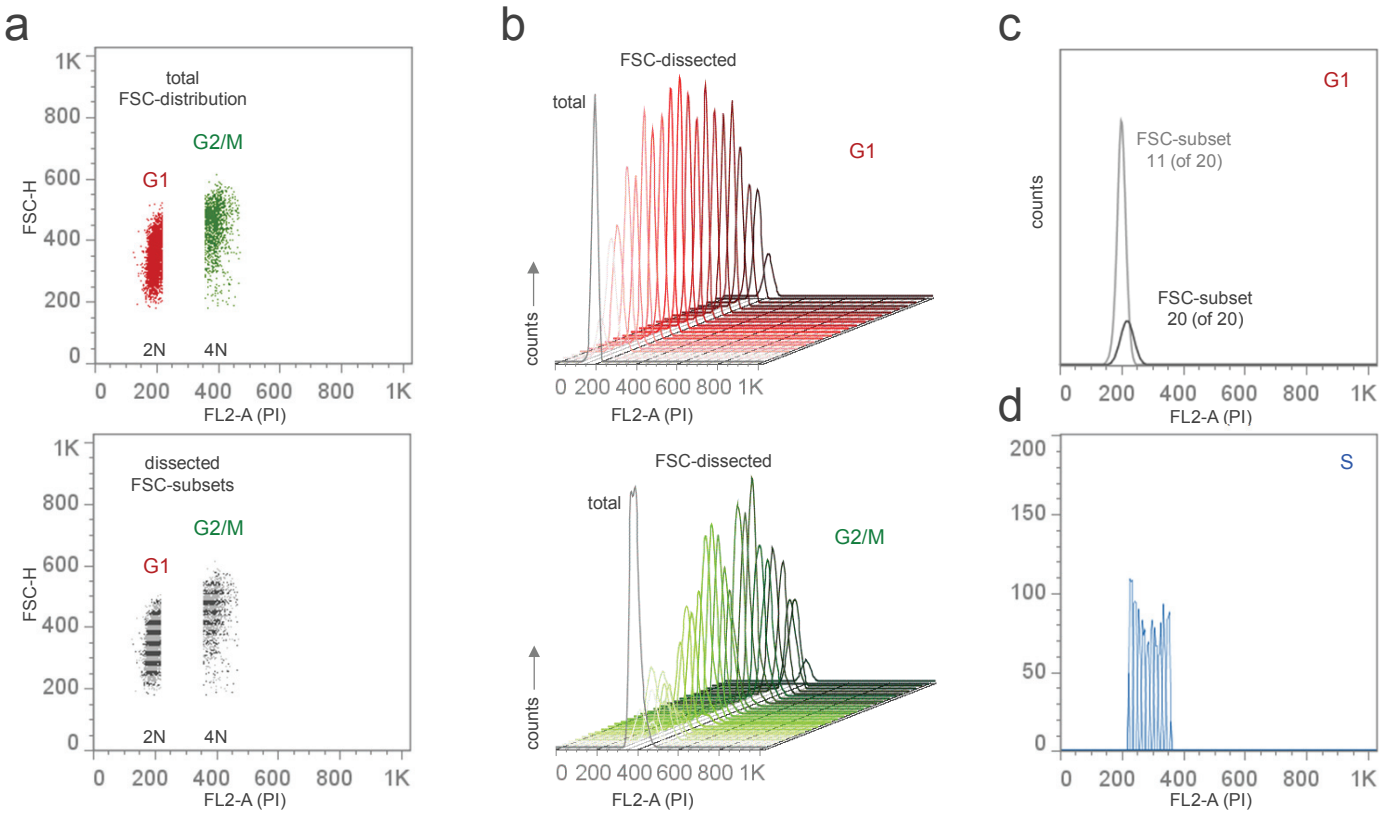

Example of a complete $FSC_{(G1)}/DNA_{(S)}/FSC_{(G2/M)}$ dissection.

(a) Dot plot depiction of G1 and G2/M subsets of propidium iodide-stained MEFs showing their total FSC distribution (*top*) and corresponding subsets obtained via FSC dissection (*bottom*). **(b)** Stagger offsets of non-dissected (*total*) versus FSC-dissected G1 (*top*) and G2/M (*bottom*) cells analysed in **a**. **(c)** DNA histogram overlay of mid (FSC subset 11 of 20) and late (FSC subset 20 of 20) G1 cells. **(d)** S phase subsets obtained via FL2-A (DNA) dissection.

Nature Protocols: doi: 10.1038/nprot.2013.011

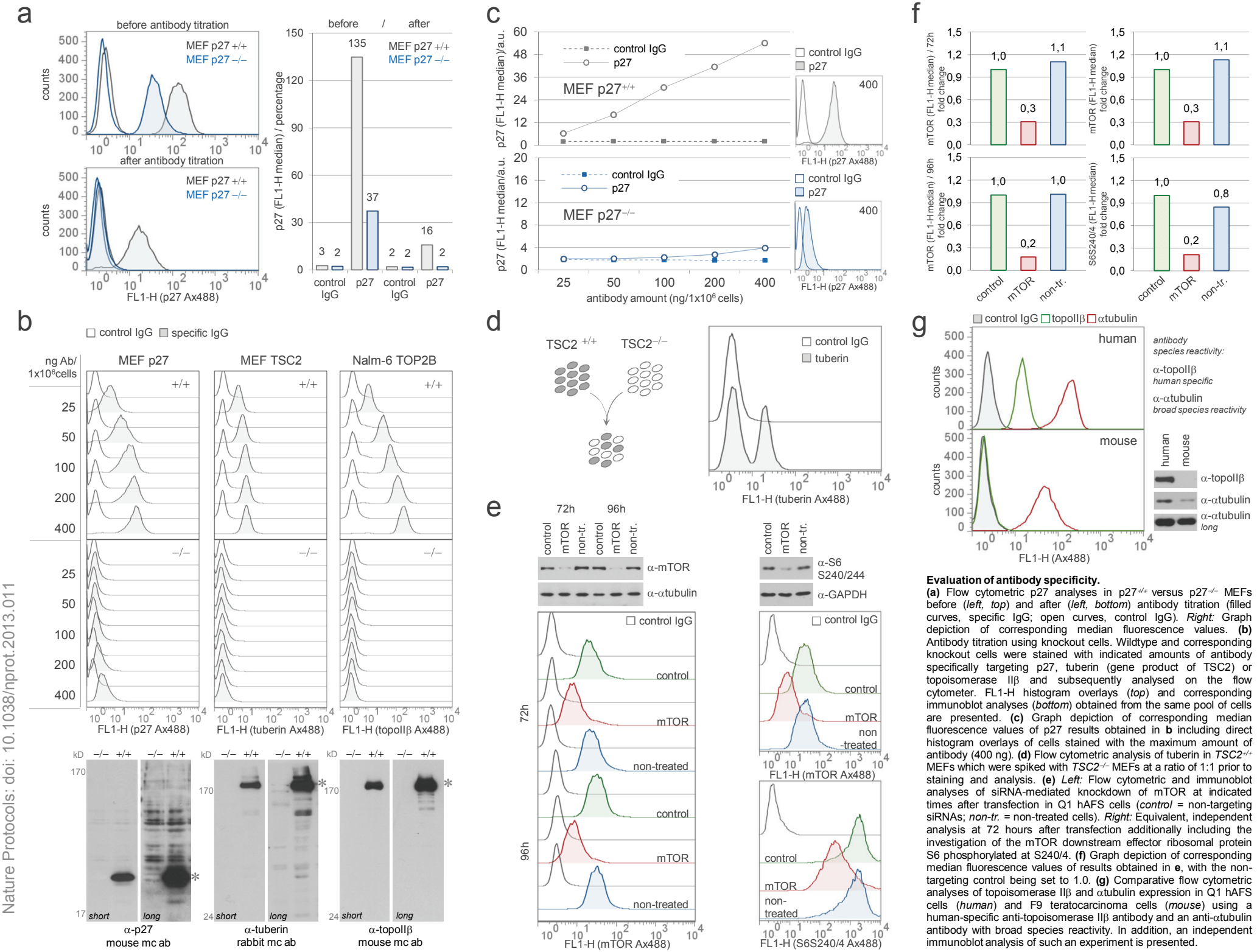

Nature Protocols: doi: 10.1038/nprot.2013.011

Evaluation of antibody specificity.
(a) Flow cytometric p27 analyses in p27$^{+/+}$ versus p27$^{-/-}$ MEFs before (*left, top*) and after (*left, bottom*) antibody titration (filled curves, specific IgG; open curves, control IgG). *Right:* Graph depiction of corresponding median fluorescence values. **(b)** Antibody titration using knockout cells. Wildtype and corresponding knockout cells were stained with indicated amounts of antibody specifically targeting p27, tuberin (gene product of TSC2) or topoisomerase IIβ and subsequently analysed on the flow cytometer. FL1-H histogram overlays (*top*) and corresponding immunoblot analyses (*bottom*) obtained from the same pool of cells are presented. **(c)** Graph depiction of corresponding median fluorescence values of p27 results obtained in **b** including direct histogram overlays of cells stained with the maximum amount of antibody (400 ng). **(d)** Flow cytometric analysis of tuberin in *TSC2*$^{+/+}$ MEFs which were spiked with *TSC2*$^{-/-}$ MEFs at a ratio of 1:1 prior to staining and analysis. **(e)** *Left:* Flow cytometric and immunoblot analyses of siRNA-mediated knockdown of mTOR at indicated times after transfection in Q1 hAFS cells (*control* = non-targeting siRNAs; *non-tr.* = non-treated cells). *Right:* Equivalent, independent analysis at 72 hours after transfection additionally including the investigation of the mTOR downstream effector ribosomal protein S6 phosphorylated at S240/4. **(f)** Graph depiction of corresponding median fluorescence values of results obtained in **e**, with the non-targeting control being set to 1.0. **(g)** Comparative flow cytometric analyses of topoisomerase IIβ and αtubulin expression in Q1 hAFS cells (*human*) and F9 teratocarcinoma cells (*mouse*) using a human-specific anti-topoisomerase IIβ antibody and an anti-αtubulin antibody with broad species reactivity. In addition, an independent immunoblot analysis of such an experiment is presented.

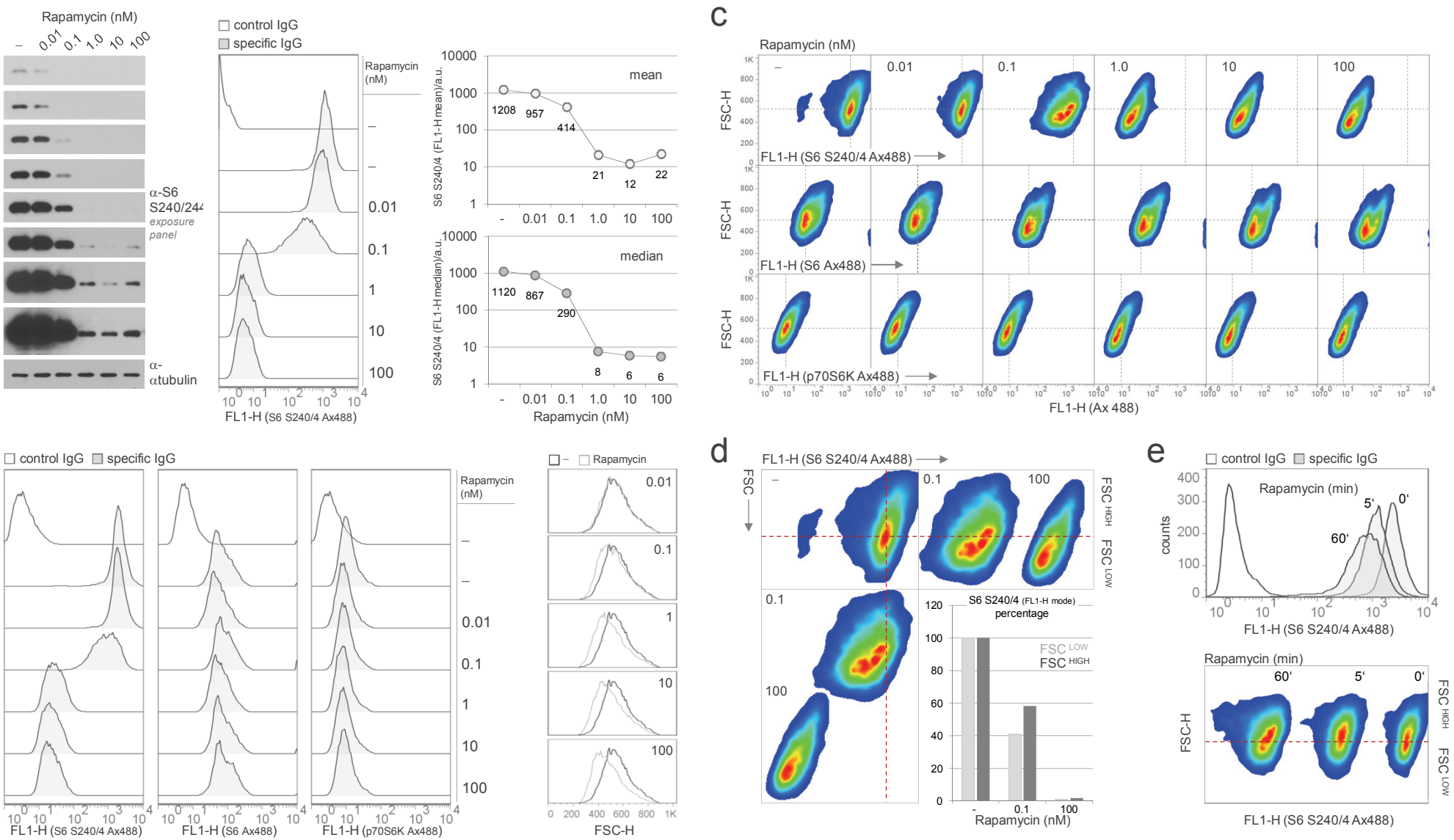

Evaluation of antibody sensitivity and the comparative analysis of flow cytometry and immunoblotting with regard to the quantifiability of obtained results.

(a) Q1 hAFS cells treated with varying amounts of Rapamycin ranging from 0.01 nM to 100 nM for 24 hours were analysed for ribosomal protein S6 phosphorylation at S240/4 via immunoblotting (*left*) and flow cytometry (*middle*). (– *Rapamycin,* DMSO-treated control cells). A total of eight different immunoblot exposures are presented to be able to evaluate concentration-dependent differences of varying extent. *Right:* Graph depiction of corresponding mean (*top*) and median (*bottom*) fluorescence values of cytofluorometrically obtained results. **(b)** Rapamycin treatments described in **a** were repeated and flow cytometric analyses of phosphorylated S6, total S6 and p70S6K were performed (*left*). In addition, FSC analyses of so treated cells are presented (*right*). **(c)** Cell size (FSC) versus protein (FL1-H) analyses of cells described in **b**. A quad gate was set into the center of each DMSO-treated population and copied to adjacent plots to better visualize FSC and FL1-H-shifts. **(d)** Focused depiction of the S6 S240/4 results presented in **c** enabling direct comparison of DMSO, 0.1 nM and 100 nM Rapamycin treated cells. To better visualize shifts in FSC and FL1-H and to roughly divide populations in cells of smaller (FSC^{LOW}) and bigger (FSC^{HIGH}) size, a red quad gate was set into the center of the DMSO-treated cells and likewise extended towards 0.1 nM and 100 nM populations for FL1-H and FSC. Included is a graph depiction of corresponding S6 S240/4 fluorescence values for the FSC^{LOW} and FSC^{HIGH} population with the corresponding DMSO-treated populations being set to 100%. **(e)** Time course experiment in which Q1 hAFS cells were treated with 100 nM Rapamycin and cytofluorometrically analysed for S6 S240/4 levels (*top*). In addition, FSC analyses of S6 S240/4 populations were performed and similarly depicted as described in **d** (*bottom*).

Nature Protocols: doi: 10.1038/nprot.2013.011

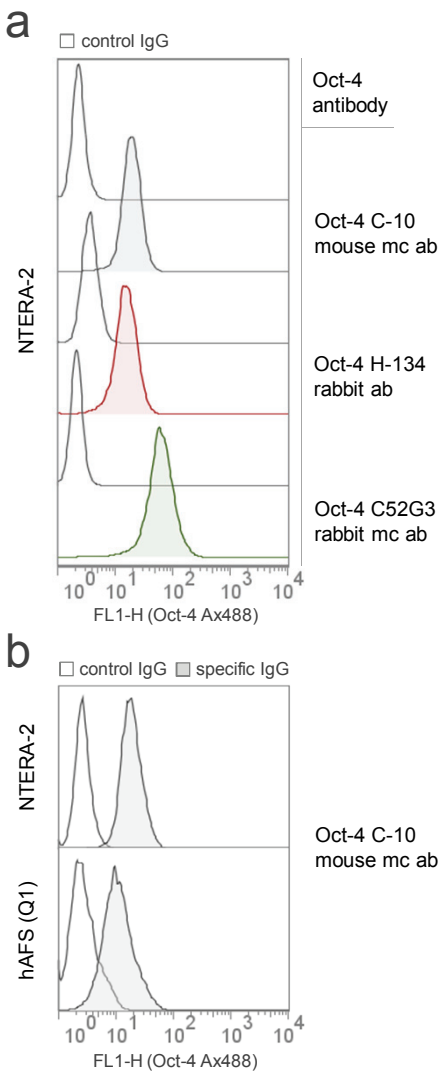

Flow cytometric Oct-4 analyses in Q1 human amniotic fluid stem (hAFS) cells and human teratocarcinoma cells.

(a) NTERA-2 human teratocarcinoma cells were stained for Oct-4 using three different, commercially available antibodies and cytofluorometrically analysed. **(b)** In an independent experiment, Q1 human amniotic fluid stem cells were co-analysed.

Nature Protocols: doi: 10.1038/nprot.2013.011

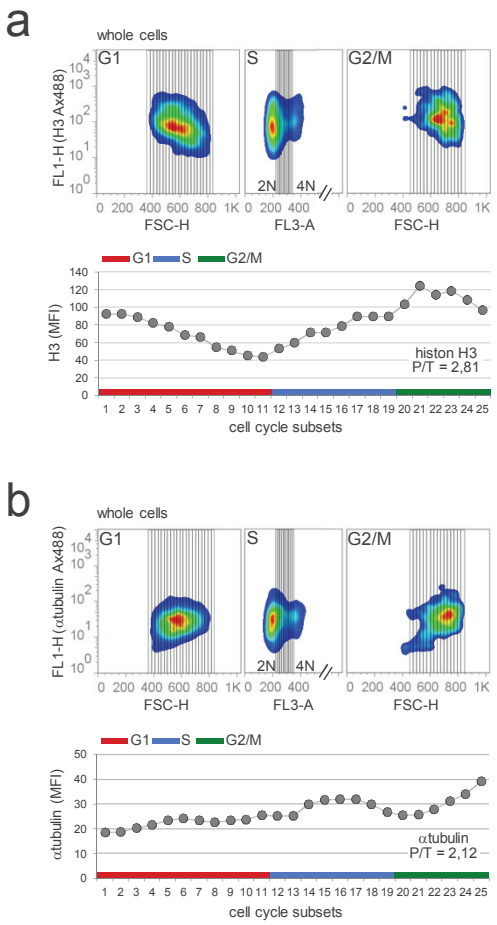

Cell cycle regulation of histon H3 (a) and αtubulin (b) in Q1 human amniotic fluid stem cells.

Top panels: Two-dimensional dot plots showing the subset-specific dissection of forward scatter (FSC-H) intensities (cell size) versus fluorescence (FL1-H) intensities (protein stain) for G1 and G2/M phase cells and of fluorescence intensities of DNA (FL3-A) versus protein (FL1-H) stains for S phase cells using a rectangular gating tool. *Bottom panels:* Contiguous depiction of dissected cell cycle subsets and their corresponding median fluorescence values (*MFI*, median fluorescence intensity) in arbitrary units (*a.u.*). The P/T (Peak-to-Trough) ratios are indicated.

Nature Protocols: doi: 10.1038/nprot.2013.011

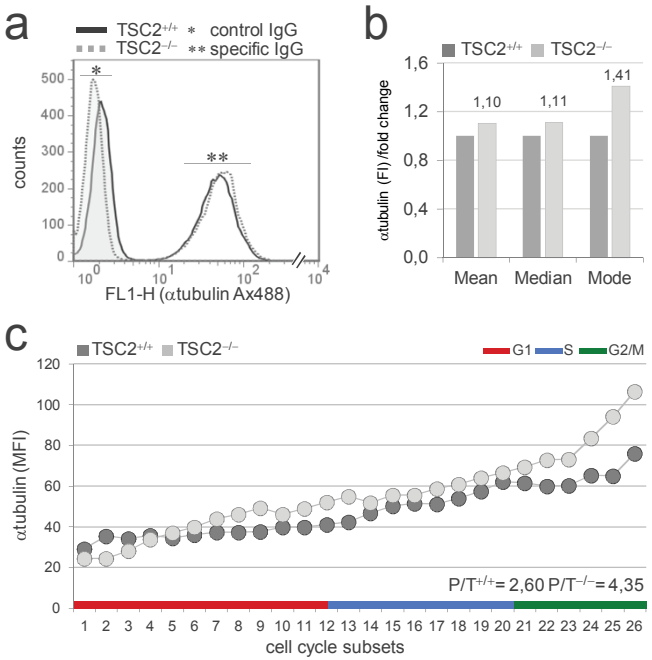

Expression and cell cycle regulation of αtubulin in *TSC2*$^{+/+}$ verus *TSC2*$^{-/-}$ MEFs.

(a) Flow cytometric analyses of αtubulin expression in *TSC2*$^{+/+}$ and *TSC2*$^{-/-}$ MEFs. Overlays of corresponding FL1-H histograms are presented. **(b)** Graph depiction of αtubulin-specific mean, median and mode (peak) fluorescence intensities (*FI*), with values for wildtype MEFs being set to 1.0. **(c)** Graph depiction of the αtubulin cell cycle regulation. *MFI*, median fluorescence intensity; P/T (Peak-to-trough) ratios are indicated.

Nature Protocols: doi: 10.1038/nprot.2013.011

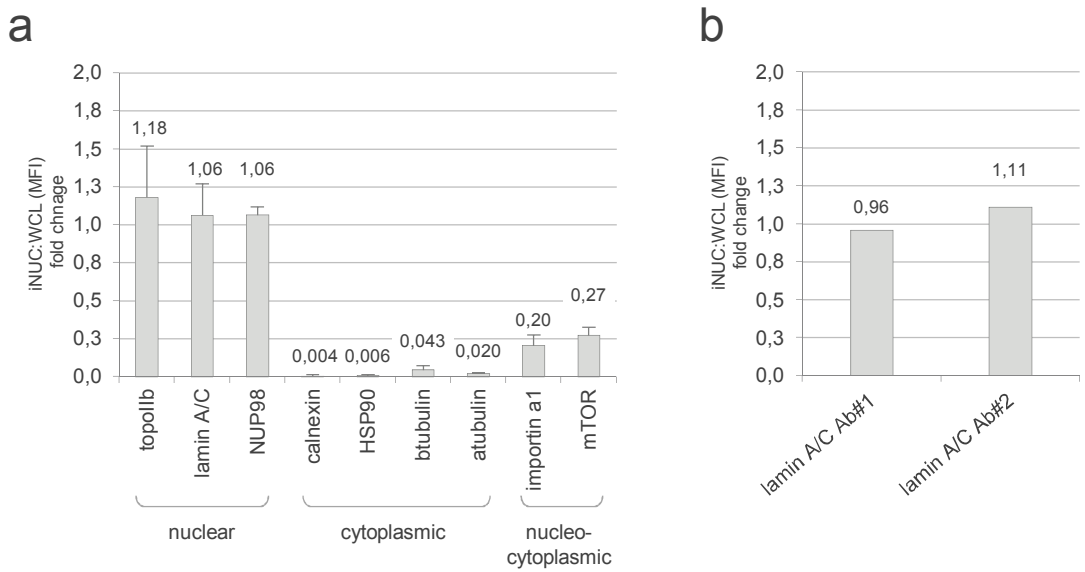

Ratios of nuclear to whole cell MFIs (FL1-H median fluorescence intensities) for cytofluorometrically analysed nuclear, cytoplasmic and nucleocytoplasmic proteins.

(a) Q1 whole cells (*WCL*) and islolated nuclei (*iNUC*) were stained for indicated nuclear, cytoplasmic and nucleocytoplasmic proteins and fluorocytometrically analysed. Obtained median fluorescence values of nuclei were divided by corresponding values derived from whole cell stainings and resulting ratios were plotted in a histogram. Results are derived from two to three independent experiments. **(b)** Equivalent analysis for the expression of lamin A/C using two different antibodies.

Nature Protocols: doi: 10.1038/nprot.2013.011

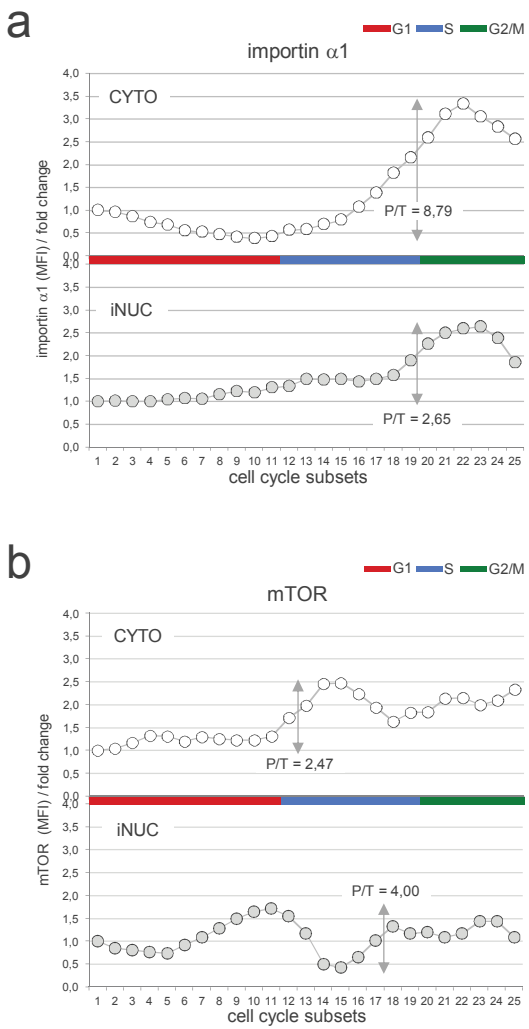

Depiction of fold changes in the cell cycle regulation of cytoplasmic versus nuclear importin α1 and mTOR.

For better comparison of fold changes in the cell cycle regulation of cytoplasmic (*CYTO*, cytoplasm) versus nuclear (*iNUC, isolated nuclei*) importin α1 **(a)** and mTOR **(b)** presented in **Fig. 7**, graphs of normalized regulations are displayed, with the very first G1 subset being set to 1.0. Corresponding P/T (Peak-To-Trough) ratios are indicated.

Nature Protocols: doi: 10.1038/nprot.2013.011

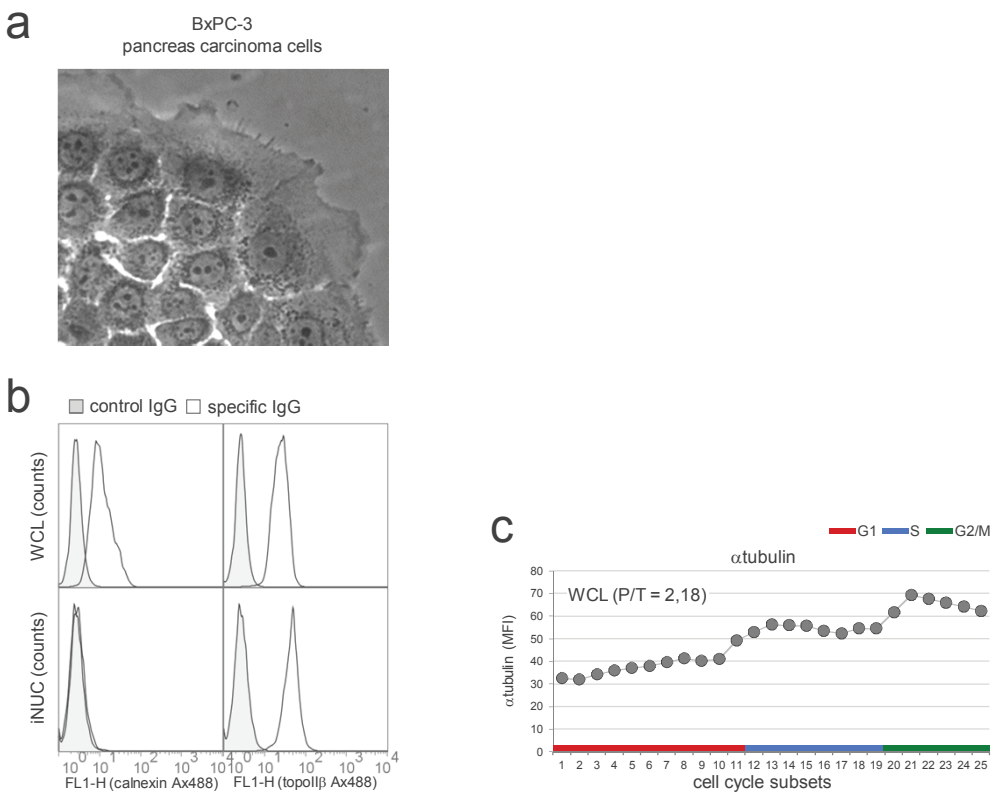

Cell cycle regulation of αtubulin in BxPC-3 pancreas carcinoma cells.

(a) Representativ picture of epithelial BxPC-3 adenocarcinoma cells growing in colony-like structures. **(b)** Flow cytometric analyses of calnexin (*left*) and topoisomerase IIβ (*right*) in whole cells (*WCL, top*) and isolated nuclei (*iNUC, bottom*). Overlays of corresponding FL1-H histograms are presented. **(c)** Whole cell analysis of the cell cycle regulation of αtubulin. P/T (Peak-to-trough) ratio is indicated.

Nature Protocols: doi: 10.1038/nprot.2013.011